Journal of Inflammation Research

Dovepress
Taylor & Francis Group

Open Access Full Text Article

ORIGINAL RESEARCH

Kuiyangling Enema Alleviates Ulcerative Colitis Mice by Reducing Levels of Intestinal NETs and Promoting HuR/VDR Signaling

Dong Zhang[1,2], Zeming Zhu[3], Zhangyou He[4], Siwei Duan[3], Qincheng Yi[4], Min Qiu[3], Xingzhen Dai[3], Guang Su[4], Kexin Li[1,2], Lin Xu[1,2], Donghou Liu[1,2], Yabin Wu[1,2], Yong Gao[3], Ruliu Li[3], Shaoju Guo[1,2]

[1]Gastroenterology Department, The Fourth Clinical Medical College of Guangzhou University of Chinese Medicine, Shenzhen, Guangdong Province, 518000, People's Republic of China; [2]Gastroenterology Department, Shenzhen Hospital of Traditional Chinese Medicine, Shenzhen, Guangdong Province, 518000, People's Republic of China; [3]Science and Technology Innovation Center, Guangzhou University of Chinese Medicine, Guangzhou, Guangdong Province, 510000, People's Republic of China; [4]Guangzhou University of Chinese Medicine, Guangzhou, Guangdong Province, 510000, People's Republic of China

Correspondence: Ruliu Li, Science and Technology Innovation Center,Guangzhou University of Chinese Medicine, No. 12, Jichang Road, Baiyun District, Guangzhou City, Guangdong Province, 510000, People's Republic of China, Tel +86-020-39357088, Email lrl@gzucm.edu.cn; Shaoju Guo, Gastroenterology Department, The Fourth Clinical Medical College, Guangzhou University of Chinese Medicine, No. 1, Fuhua Road, Shenzhen City, Guangdong Province, 518000, People's Republic of China, Tel +86-0755-82571384, Email gsj1080@163.com

Purpose: Kuiyangling is a traditional Chinese medicine formula used for the treatment of ulcerative colitis, but the specific mechanism remains unclear. Imbalance in NETs regulation is one of the important factors contributing to the onset of ulcerative colitis (UC). The HuR/VDR signaling pathway plays a significant role in restoring the intestinal mucosal barrier in UC. The aim of this study is to explore the mechanism of Kuiyangling in the treatment of ulcerative colitis.

Methods: A mouse model of ulcerative colitis using 3% DSS water was considered, and model, normal, Kuiyangling medium- (5 $g \cdot kg^{-1}$) and high-dose (10 $g \cdot kg^{-1}$), and mesalazine (50 $mg \cdot kg^{-1}$) groups were created. Measurements of colon length, spleen index, histopathological variances, subcellular structure observations, ROS content, and NET-related proteins (PAD4, MPO, citH3) were obtained through HE staining, electron microscopy, live imaging, and Western blotting assays. Immunohistochemistry and immunofluorescence analyses were conducted to assess the levels of HuR/VDR protein complex, ZO-1, Occludin, Claudin-7, and intestinal NETs. An ELISA kit was utilized to determine cytokine levels, LC-MS was performed to analyze the composition of Kuiyangling, and next-generation sequencing was conducted for detection of the intestinal mucosal transcriptome.

Results: Kuiyangling reduced DAI, splenic index, and ROS content; maintained mucosal structure; decreased inflammation; and increased colon length and body mass index. Western blotting indicated that Kuiyangling reduced PAD4,MPO, and citH3 levels. Kuiyangling decreased NETs and increased the expression levels of ZO-1, Occludin, and Claudin-7, as well as up-regulating HuR, VDR, and HuR/VDR proteins. Kuiyangling reduced IL-1β, IL-6, and TNF-α levels while increasing TGF-β, IL-10, and IL-37 levels. Kuiyangling reduced inflammatory response proteins and elevated the levels of anti-inflammatory and intestinal barrier proteins, possibly inhibiting the TNF and oxidative phosphorylation signaling pathways.

Conclusion: Kuiyangling enema in treating ulcerative colitis in mice, associated with a reduction in intestinal NETs and enhancement of HuR-mediated intestinal barrier signaling pathways.

Keywords: ulcerative colitis, enema therapy, neutrophil extracellular traps, Chinese medicine, inflammation

Introduction

Ulcerative colitis (UC) is a chronic, non-specific inflammatory disorder primarily affecting the colonic mucosa and submucosa.[1] It is characterized by diarrhea, abdominal pain, and mucopurulent stools, posing significant global challenges due to its recurrent, lifelong course and incurability in severe cases.[2,3] The incidence of UC exceeds 7.6–8.4 per 100,000 annually and is steadily increasing.[4] Approximately 9–10% of UC-related deaths are attributed to colorectal cancer.[5] While the exact pathogenesis remains unclear, UC progression is linked to dysregulated intestinal

Received: 21 September 2024
Accepted: 21 December 2024
Published: 8 January 2025

Graphical Abstract

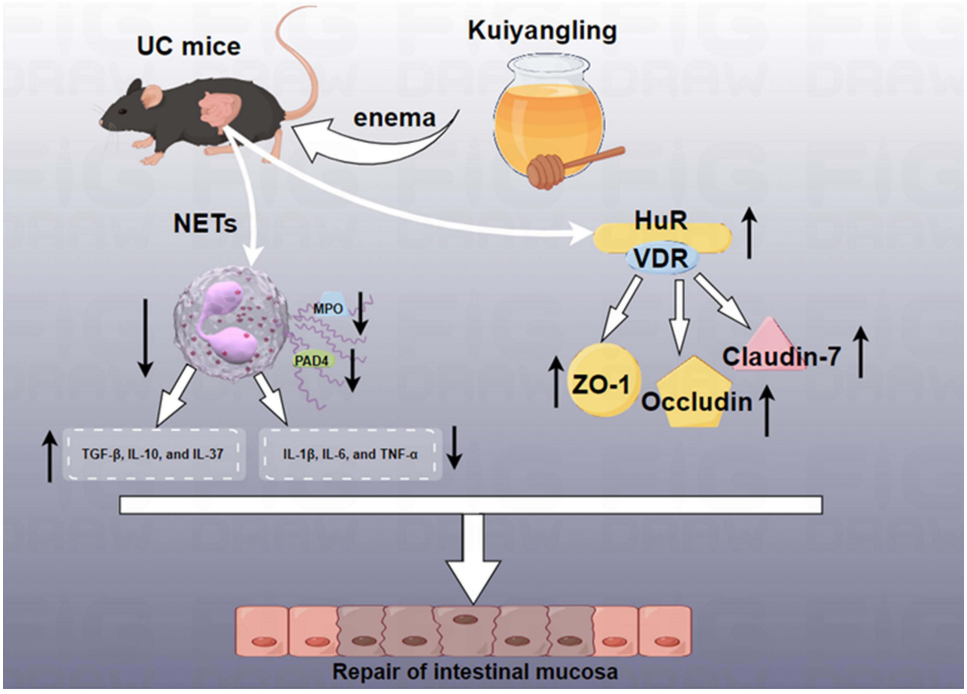

immunity, microbial imbalances, and environmental, genetic, and psychological factors.[6] Current treatments, including aminosalicylates, immunosuppressants, corticosteroids, and biologics, are often limited by suboptimal efficacy, high costs, and adverse effects, such as nausea, Cushing's syndrome, and bone marrow suppression.[7,8] Notably, 50% of moderate-to-severe UC cases fail to achieve satisfactory outcomes following standard therapy.[9] Thus, advancing understanding of UC pathogenesis and developing more effective treatments remain critical.

Neutrophil extracellular traps (NETs), first described in 2004, are extracellular structures designed to trap and eliminate bacteria.[10] This process is accompanied by a specialized form of neutrophil death, termed "NETosis".[11] Dysregulation of NETs contributes to exacerbated inflammation, malignant metastasis, and thrombosis.[12] Evidence suggests that neutrophil infiltration in intestinal mucosa correlates directly with the severity of inflammatory bowel disease (IBD).[13–15] Elevated levels of neutrophil markers, such as PTX3, neutrophil gelatinase B, and MMP-9, are observed in the sera of active IBD patients compared to healthy controls, and NET components are detectable in stool samples of IBD patients, decreasing with certain treatments.[16] NET-associated proteins are overexpressed in the colons of ulcerative colitis (UC) patients. NET formation can be induced by TNF-α and ERK1/2 activation, which further upregulates pro-inflammatory cytokines such as TNF-α and IL-1β. Inhibition of NET release has been shown to mitigate colonic inflammation in mouse models.[16] Additionally, DDIT4/REDD1 complexes have been implicated in promoting NET formation and mediating UC-specific inflammation.[17] These findings highlight NETs as a critical therapeutic target in UC management.

Evidence-based clinical studies have demonstrated the unique benefits of Traditional Chinese Medicines (TCMs) in managing ulcerative colitis (UC), including symptom alleviation, remission induction, relapse prevention, quality of life improvement, and complication reduction.[18] TCMs have been shown to target UC through multiple mechanisms, such as anti-inflammatory effects, immune modulation, and mucosal repair.[19]

HuR, a well-studied RNA-binding protein (RBP), is significantly expressed in intestinal epithelial cells and plays a key role in maintaining epithelial homeostasis.[20] Inflammatory bowel disease (IBD) patients exhibit reduced HuR expression in the intestinal mucosa.[21] HuR primarily binds to AU-rich elements (AREs) in the 3′-untranslated region of

target mRNAs to regulate their stability but can also bind selectively to AREs in the 5′-untranslated region to control mRNA stability and translation.[22,23] As a critical post-transcriptional regulator, HuR mediates gene expression responses to environmental stress and interacts with non-coding RNAs (ncRNAs) to regulate target genes.[22] In intestinal epithelial cells (IECs), HuR knockdown inhibits the Wnt signaling pathway, impeding mucosal renewal, and suppresses CDC42 expression, hindering epithelial repair after injury.[24,25] Moreover, HuR absence reduces intestinal tumor incidence by modulating protein expression levels and maintains epithelial homeostasis through interactions with microRNAs (miRNAs).[22] These findings underscore HuR's essential role in intestinal epithelial integrity and its potential as a therapeutic target.

The vitamin D receptor (VDR), a nuclear receptor highly expressed in intestinal epithelial cells, mediates the actions of active vitamin D.[26] Upon binding with vitamin D3, activated VDR forms a heterodimer with retinoid X receptors and directly interacts with vitamin D-responsive elements in target gene promoters, enhancing gene transcription.[26] Emerging evidence highlights the crucial role of VDR in intestinal mucosal maturation, barrier integrity, innate immunity, epithelial host defense, and interactions with the luminal microbiota.[27] VDR activation protects intestinal epithelial cells from bacterial infections and mitigates mucosal inflammation, injury, and erosion.[28] Targeted VDR deficiency in intestinal epithelial cells impairs Paneth cell function and suppresses autophagy in the colonic mucosa of mice with colitis.[29] Alterations in VDR levels in intestinal tissues are associated with pathologies such as inflammatory bowel disease (IBD), cancer, and chronic infections.[30] In both mice and patients with infectious diseases, lower VDR abundance correlates with increased chronic mucositis.[31]

Studies have shown that while HuR silencing does not affect overall VDR mRNA levels, it inhibits VDR translation by interacting with the 3′-untranslated region of VDR mRNA.[32] The reduced levels of HuR and VDR observed in the inflamed and injured mucosa of IBD patients suggest that disruption of the HuR/VDR regulatory pathway contributes to inflammation-related mucosal diseases.[33] Notably, VDR regulates the expression of intestinal barrier proteins, including ZO-1, Occludin, and Claudin-7, indicating that HuR influences these proteins' expression via VDR modulation.

Kuiyangling, a traditional Chinese medicine enema formula, comprises *Sophora flavescens Aiton* (Kushen), Acacia catechu (Ercha), *Panax notoginseng* (Sanqi), *Bletilla striata* (Baiji), *Typha angustifolia* (Puhuang), *Robinia pseudoacacia* (Huaihua), *Baphicacanthus cusia* (Qingdai), *Melaphis chinensis* (Wubeizi), and *potassium alum* (Baifan), as detailed in Table 1. Previous studies by our group have demonstrated that Kuiyangling significantly alleviates symptoms in patients with active ulcerative colitis (UC), primarily by mitigating intestinal inflammation, though the precise mechanism remains unclear.[34–37] This research suggests that Kuiyangling may exert therapeutic effects by reducing the production of neutrophil extracellular traps (NETs). This study has shown that Kuiyangling alleviates UC symptoms by decreasing NET production and inhibiting the TNF and oxidative phosphorylation signaling pathways. Moreover, Kuiyangling not only reduces NET levels but also enhances HuR/VDR signaling, upregulates intestinal barrier proteins, and mitigates intestinal inflammatory responses, thereby promoting mucosal repair.

Table 1 The Information of Herbs in Kuiyangling

Chinese Pinyin Name	Academic Name	Place of Origin	Part of Medicine	Weight (g)	Batch Number
Kushen	*Sophora flavescens* Aiton	Guangxi, China	Root	30g	2104001
Ercha	*Acacia catechu* (L.f.) Willd.	Yunnan, China	Branch	15g	2106159
Sanqi	*Panax notoginseng* (Burkill) F.H.Chen	Yunnan, China	Root	10g	2102018
Baiji	*Bletilla striata* (Thunb.) Rchb.f.	Yunnan, China	Root	15g	20110012
Puhuang	*Typha angustifolia* L.	Hebein,China	Pollen	15g	210360841
Huaihua	*Robinia pseudoacacia* L	Jiangsu,China	Bud	15g	202001
Qingdai	*Baphicacanthus cusia* (Nees) Bremek	Sichuan, China	Leave	10g	191205701
Wubeizi	*Melaphischinensis* (Bell) Baker	Guangxi,China	Gall	10g	2106110
Baifan	$KAl(SO_4)_2 \cdot 12H_2O$	Anhui, China	KAl(SO4)2–12H2O	10g	2102612

https://doi.org/10.2147/JIR.S492818

Materials and Methods

Preparation of Drugs

The herbal composition of Kuiyangling is detailed in Table 1. The herbs were purchased from Kangmei Pharmacy (Guangzhou, China). First, 130 g of Kuiyangling was immersed in 1300 mL of pure water for 1 hour. The herbs were then boiled for 1 hour and filtered; this step was repeated once. A rotary evaporator was used to concentrate the collected filtrate to 800 mL. Finally, the concentrated filtrate was frozen and dried, then stored in a refrigerator at −20 °C. The 130 g of Kuiyangling eventually yielded 33.3 g of lyophilized powder, with a yield rate 25.6%.

UPLC-MS

Ginsenoside Rg1 (Batch No. MUST-22110110), Ginsenoside Rb1 (Batch No. MUST-23010710), *Panax ginseng* saponin R1 (Batch No. MUST-22110110), Psoralenoside (Batch No. MUST-22110812), Catechin (Batch No. MUST-22072709), Indoleucine (Batch No. MUST 22103114), Quercetin (Batch No. MUST-22042012), Gallic Acid (Batch No. MUST-22112411), Epigallocatechin (Batch No. MUST-22050817), Epicatechin (Batch No. MUST-22062410), and Isorhamnetin-3-O-Neohesperidin (Batch No. MUST-22081313) were purchased from Chengdu MUST Biotechnology Co., Ltd., China (all with mass fraction ≥ 98%). Control Picrasidine (Batch No. 110805-202010), Oxidized Picrasidine (Batch No. 110780–202210), Sophora Ficusine (Batch No. 112052-202001), Oxidized Sophora Ficusine (Batch No. 111652-202202), and Rutin (Batch No. 100080 Rutin (Lot No. 100080–202012) were purchased from the China Academy of Food and Drug Control (all with mass fraction ≥ 98%). An appropriate amount of the above standard control products was taken, and they were dissolved in 70% methanol and water to make up a 100 μg/mL control stock solution.

Next, we took 50 μL of Kuiyangling extract solution and diluted it with 1 mL of methanol. The resulting solution was vortex mixed for 3 min, centrifuged at 14,000 rpm for 15 min, and the supernatant was taken to obtain the test solution. The standard was dissolved in 70% methanol and water to produce a 100 μg/mL mixture.

The chromatographic conditions were as follows: Waters Acquity UPLC BEH C18 column (100 mm × 2.1 mm, 1.7 μm). The mobile phase was 0.01% formic acid acetonitrile (A)–0.01% formic acid in water (B), and the gradient elution program was 0–4.5 min, 5–20% A; 4.5–8.0 min, 20–60% A; 8.0–9.0 min, 60–80% A. Separation was performed on an HPLC column (100 mm × 2.1 mm, 1.7 μm). The gradient elution program was 0–4.5 min, 5–20%A; 4.5–8.0 min, 20–60%A; 8.0–9.0 min, 60–80%A; 9.0–9.2 min, 80–100%A. The column temperature was 50 °C, the flow rate was 0.4 mL/min, and the injection volume was 2 μL.

The mass spectrometry conditions were as follows: Waters Xevo G2 Q-Tof mass spectrometer with electrospray ion source for positive and negative ion modes, capillary voltage of 2.8 kV (−3.0 kV), cone bore voltage of 40 V (−40 V), ion source temperature of 150 °C, de-solventizing gas temperature of 500 °C, de-solventizing gas flow rate of 900 L/h, and a scanning range of m/z 100–1200.

Data were analyzed using the UNIFI software in combination with the instrument's own database of chemical constituents of traditional Chinese medicines. The structures were determined based on precise molecular weight and secondary mass spectrometry information, confirmed through manual screening.

Ethics Statement and Animal Experiment

The dataset GSE225420 (https://www.ncbi.nlm.nih.gov/geo/query/acc.cgi?acc=GSE225420) used in our study, sourced from the GEO database, was uploaded by our research group after sequencing mouse intestinal mucosal tissue. This study does not involve research on humans.

All animal trials were implemented in rigorous accordance with the NIH's (publication #85-23, revised in 1985) instructions with respect to the care and usage of lab animals, and were supported by the Animal Ethics Committee of Guangzhou University of Traditional Chinese Medicine (ethics approval number, 20210903008).

C57BL/6J mice at 7 weeks were purchased from Zhuhai Biotech Co., Ltd. (Zhuhai, Guangdong). The animal license number was as follows: SYXK (Yue) 2020–0051. Adaptive feeding took place for 10 days. We estimated the dosage of lyophilized powder of Kuiyangling according to the effective dosage of Kuiyangling in clinical practice considering a standard weight of 60 kg for adults, and the result was 0.56 g/kg. In accordance with the methods of Chinese medicine

and pharmacological research, we converted the human dose into the dose of 5.0 g/kg for mice according to the body surface area, which was used as a reference standard to design the dosage of 10 g/kg. According to their body weight, mice were split into 5 groups at random: 10 in the normal group, 14 in the model group, 14 in the middle-dose Kuiyangling group (5 g/kg), 14 in the high-dose Kuiyangling group (10 g/kg), and 14 in the mesalazine group (50 mg/kg). The normal group was given pure water for drinking, while the other groups were given 3% DSS (MP Biomedicals, lot # 9011–18-1) for free drinking for 7 days. At the same time, drug treatment was carried out. The mice were subjected to drug enema under 300 mL/min isoflurane anesthesia. The enema volume reached 0.2 mL; in addition, the time of retention was 10 min. The daily body weight, blood index in stool, and stool characteristics of rats in every group were measured. The DAI (disease activity index) of the mice in each group was obtained as follows: DAI = (score of body mass reduction + score of stool characteristics + score of blood in stool)/3. The spleen index was measured as Spleen index = spleen mass/mouse body weight, which is positively correlated with peripheral inflammatory reactions. On the seventh day of the experiment, mice were euthanized under isoflurane anesthesia, the colon was removed, its length was recorded, the intestinal mucosa was scraped, and peripheral serum was separated. In addition, part of the intestinal tissue was fixed with 2.5% glutaraldehyde or 4% paraformaldehyde. The DAI scoring criteria are detailed in Table 2.

Detection of Blood Index in Stool

Fecal occult blood test reagent (Colloidal Gold Method) (Zhuhai Beso Biotechnology Co., Ltd., Zhuhai, China) was used to detect the degree of fecal occult blood presentation in mice. An appropriate amount of stool was applied to the test paper, and then working solution A and working solution B were added separately. After this, the color results were determined within 2 min. The degree of stool blood was proportional to the color shade of the test paper. Sample size> 5. This experiment was performed as a separate, independent experiment.

HE Staining

The intestinal tissues fixed in 4% paraformaldehyde were de-waxed in xylene for 10 min. The samples were then placed in 95%, 85%, and 70% gradient ethanol for 5 min each for sample hydration. After hydration, the samples were rinsed 3 times in PBS, lasting 5 min each. Moreover, they were stained with hematoxylin stain for 10 min, followed by fractionation with 1% ethanol hydrochloride. The tissue sections were then dehydrated in a gradient of ethanol solution, and the samples were sealed and air-dried for photography. The intestinal pathological injury scoring criteria are detailed in Table 3. Sample size = 5. This experiment was performed as a separate, independent experiment.

Table 2 DAI Scoring Criteria

Scoring Item	Stool Consistency Score	Rectal Bleeding Score	Body Weight Loss Score
0 points	Normal	No blood	No weight loss
1 point	Soft or slightly loose	Trace blood	Mild weight loss (0–5%)
2 points	Loose or mucous	Moderate blood	Moderate weight loss (5–10%)
3 points	Very loose or watery	Large amount of blood	Significant weight loss (10–15%)

Table 3 Intestinal Pathological Scoring Criteria

Score	Inflammatory Cells Infiltration	Depth of Invasion	Crypt Injury	Pathological Range (%)
0	None	None	None	0
1	±	Mucosa layer	1/3	1–25
2	+	Mucosa and submucosa	2/3	26–50
3	++	Full	Full	51–75
4	+++			76–100

https://doi.org/10.2147/JIR.S492818

Electron Microscopic Observation

The intestinal tissues of mice were fixed with 2.5% glutaraldehyde and observed using Zeiss transmission electron microscopy. The samples were healed using ethanol, dropped onto a copper grid on carbon film, and subsequently dried. The working voltage was modulated to 75 kV, and the filament current was switched to the locked position. An appropriate field of view was selected, and the brightness was adjusted and focused to capture images. Sample size = 1. This experiment was performed as a separate, independent experiment. Due to limitations in funding, time, and resources, only one experiment was conducted.

In vivo Imaging of Intestinal ROS

Luminol (MedChemExpress, CAS #521-31-3) was dissolved in corn oil containing 10% DMSO. Under isoflurane gas anesthesia, luminol was injected intraperitoneally and, 30 min later, the mice were euthanized to remove the intestine and placed under a PE IVIS Spectrum in vivo imager for imaging. Sample size = 5. This experiment was performed as a separate, independent experiment. Due to limitations in funding, time, and resources, only one experiment was conducted.

Western Blot Assay

Information on all the antibodies in this study is as follows: PADI4 antibody (Proteintech, Cat No: 17373-1-AP); MPO antibody (Proteintech,Cat No: 22225-1-AP); citH3 antibody (Abcam,Cat No: ab281584); GAPDH antibody (Proteintech, Cat No: 60004-1-Ig); HuR antibody (Proteintech,Cat No: 11910-1-AP); VDR antibody (Affinity,Cat No: AF6159); Occludin antibody (Proteintech,Cat No: 27260-1-AP); ZO-1 antibody (Proteintech,Cat No: 21773-1-AP); Claudin 7 antibody (Abcam,Cat No: ab27487). The colonic mucosa was homogenized and lysed with RIPA (containing 1% PMSF, Beyotime, Shanghai, China) for 30 minutes, then centrifuged at 12,000 r/min for 20 minutes at 4 °C. The supernatant BCA (Beyotime, Shanghai, China) was adopted to determine the total protein concentration. Next, 30 μg of protein was sampled and 10% SDS-PAGE gel electrophoresis was performed. After completion of electrophoresis, the protein was transferred from the gel to PVDF membrane using a semi-dry transfer method, and 5% skimmed milk was used to seal the gel. The primary antibody (1:1000) was incubated overnight, and the secondary antibody was incubated after rinsing with TBST. The strips were placed in an ECL luminescence reagent (Bio-rad, USA) and developed through exposure under a developer. The ImageJ software was used to analyze the grayscale values of the strips. Sample size =1. This experiment was performed as a separate, independent experiment. I am unable to conduct additional experiments at this time due to constraints related to resources. While I recognize that this limits the scope of my findings, I would like to emphasize that the Western blot experiment I conducted was rigorously designed and carefully executed to ensure the validity of my results. I have also included a discussion of the limitations of my study, including the lack of multiple experiments, in the discussion section.

Immunohistochemical Testing

Tissue sections were routinely de-waxed to water, then subjected to heat-mediated antigen retrieval using either a sodium citrate buffer (pH 6.0) or EDTA (pH 9.0). Sections were incubated with endogenous peroxidase blocking agent for 10 minutes. HuR (1:500), VDR (1:200), Claudin-7 (1:100), Occludin (1:200), and ZO-1 (1:200) were added dropwise and incubated overnight at 4 °C. Signal enhancement solution was incubated for 20 minutes at 37 °C. Secondary antibody was incubated for 20 minutes at 37 °C. DAB staining was visualized under a microscope. Hematoxylin was counterstained for 10 seconds. Finally, the sections were dehydrated and sealed with transparent resin. Sample size = 5. This experiment was performed as a separate, independent experiment.

Immunofluorescence Double Staining

After de-waxing the paraffin sections, proteinase K was added dropwise and incubated for 30 minutes at 37 °C to repair the tissue, followed by washing three times with PBS for five minutes each time. TUNEL reagent was added and incubated for 2 h at 37 °C, followed by washing three times with PBS lasting for five minutes each time. Then, 3% BSA

was added at a normal temperature for 30 min. Antibodies were immediately mixed in equal proportions. The mixed antibody drops were added to the specimens and incubated overnight at 4 °C in a refrigerator. The next day, the specimens were washed three times using PBS for five min each time, and incubated with secondary antibodies for one hour at normal temperatures. The DNA was stained with DAPI, incubated for 10 min, protected from light, and rinsed three times with PBS for five min each time. Sections were sealed using an anti-fluorescence quenching agent. Finally, the specimens were photographed using a fluorescence microscope. The intensity of fluorescence values using antibody and DNA co-localization staining indirectly reflected the NETs or HuR/VDR complex contents. Sample size = 5. This experiment was performed as a separate, independent experiment.

Transcriptomics Analysis

The collected intestinal mucosal tissues were sent to Shanghai OE Biotech (Shanghai, China) for transcriptome sequencing. The experimental part of the transcriptome project RNA-seq process included the following: Sample quality testing, double-stranded cDNA synthesis, transcriptome library construction, quality control, and sample up-sequencing. The obtained data were corrected and analyzed with GO, KEGG, and GSEA using the R software. Sequencing raw data from this study have been uploaded into the GEO database (GSE225420).

ELISA Analysis

Blood was collected and left to stand at a normal temperature for 1 h, then centrifuged at 3000 r/min in a centrifuge for 15 minutes at 4 °C. The supernatant was then extracted. The levels of serum IL-1β, TNF-α, IL-6, TGF-β, IL-10, and IL-37 were measured following the guidelines of the ELISA kit (Jiangsu Meimian Industrial Co., Ltd). Sample size = 5. This experiment was performed as a separate, independent experiment.

Statistics

SPSS 21.0 software was specifically chosen for conducting the statistical analysis of the gathered measurements due to its comprehensive suite of tools for handling various types of data. GraphPad Prism 7.0 was then utilized to create detailed and visually appealing statistical graphs that facilitated easy interpretation of the results.The measures were presented in a standardized format, specifically as the mean ± standard deviation (mean ± SD), to provide a clear indication of both the central tendency and variability of the data. For intergroup comparisons, the statistical analysis was tailored to the distribution of the data. When the measures followed a normal distribution, either the *t*-test or analysis of variance (ANOVA) was employed. The *t*-test was specifically used for comparisons between two groups, offering a straightforward way to determine whether there was a statistically significant difference between their means. On the other hand, ANOVA was applied for comparisons among multiple groups, allowing for the simultaneous analysis of variance between and within groups. When the data did not conform to a normal distribution, the non-parametric rank-sum test was utilized. This test does not assume a specific distribution for the data and is therefore more robust in situations where the data is not normally distributed. For categorical statistical data, the chi-square test was employed. This test is commonly used to determine whether there is a statistically significant difference between the observed and expected frequencies in one or more categories. Finally, a P-value less than 0.05 was considered to indicate a statistically significant difference between the groups, providing a clear threshold for determining whether the results were likely to be due to chance or to a real underlying effect.

Results

Kuiyangling Can Reduce the Inflammatory Response in UC Mice

From day 1 to day 3 after the start of modeling, the weight loss in the model group gradually differed from that of the normal group, but was not obvious compared with the Kuiyangling group. The DAI index was used to evaluate the changes in the physical signs of the mice (Figure 1A). The DAI index of the model group intensified gradually over the entire experimental period. Compared with the model group, the increase rate in the Kuiyangling-administered groups was evidently lower, when compared with that in the model group (Figure 1B). With the exception of the normal group,

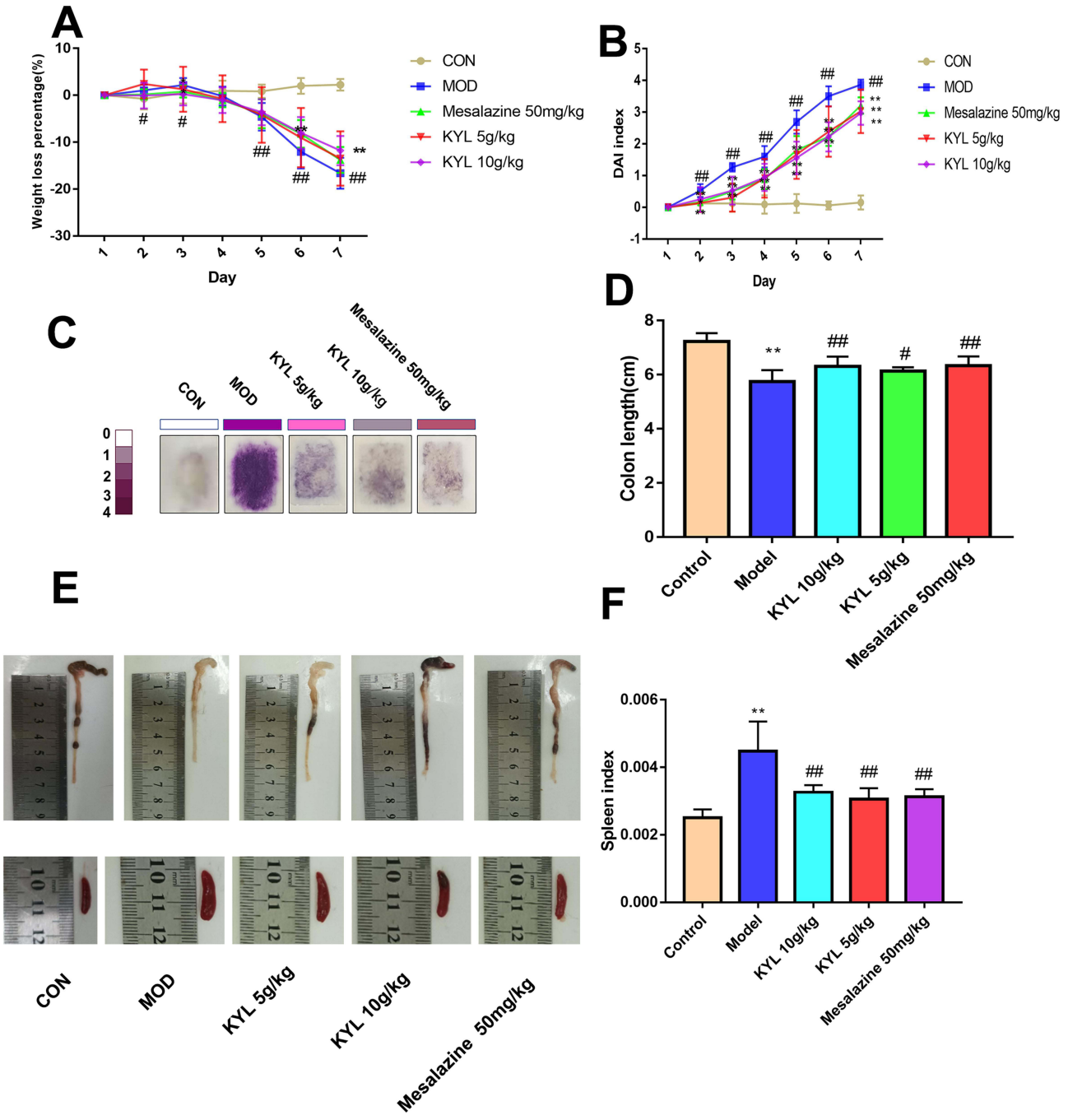

Figure 1 Kuiyangling can treat mice with ulcerative colitis. (**A**) Weight loss rate for each group. (**B**) Disease activity index (DAI) for each group. (**C**) The degree of blood in stool for each group. (**D**) and (**E**) Colon length for each group. (**D**) and (**F**): Spleen index for each group. CON, normal group; MOD, model group; Mesalazine 50 mg/kg, mesalazine 50 mg/kg group; KYL 5 g/kg, Kuiyangling 5 g/kg group; KYL 10 g/kg, Kuiyangling 10 g/kg group (*, $P < 0.05$ compared with the normal group; **, $P < 0.01$ compared with the normal group; #, $P < 0.05$ compared with the model group; # #, $P < 0.01$ compared with the model group).

the model and Kuiyangling groups exhibited an increase in DAI on day 4 compared with the first 3 days, indicating that day 4 may be an important time point in the 3% DSS modeling process. The color of the stool blood test paper was directly proportional to the amount of blood in the stool and, thus, the test paper semi-quantitatively reflects the degree of blood in the stool (Figure 1C). We selected feces on day 4 for testing. We observed that the blood in the model group was more severe, compared with that in the normal group. The blood degree in the stool was lower in the Kuiyangling group, in comparison with the model group. The colon length was negatively correlated with the degree of inflammatory

 https://doi.org/10.2147/JIR.S492818

response. In addition, the spleen index was actively linked to the inflammatory response. The shorter intestinal length and higher spleen index in the model group, when compared to the normal group, indicated a higher inflammatory response, while the longer intestinal length and lower spleen index in the Kuiyangling group, compared to the model group, indicated that the treatment significantly improved the intestinal inflammatory response (Figure 1D–F). The results indicate that the treatment design was successfully modeled, and Kuiyangling treatment yielded a significantly reduced inflammatory response in UC mice. The impact of treatment with mesalazine was similar to that of Kuiyangling.

Identification of Compounds in Kuiyangling

A total of 115 compounds were identified in the composition of Kuiyangling with UPLC-MS. Validation was carried out for the constituents represented by gallic acid, picric acid, locustine, oxidized locustine, oxidized picric acid, epigallocatechin, catechin, epicatechin, rutin, chamomile neosporin, isorhamnetin-3-O-neohesperidin, *Panax notoginseng* saponin R1, ginsenoside Rg1, quercetin, ginsenoside Rb1, and indirubin. The results are detailed in Supplementary Table 1 and Supplementary Figure 1.

Kuiyangling Can Maintain the Normal Intestinal Structure of UC Mice

HE staining revealed that the epithelial and glandular structures of the colon were intact and undamaged in the normal group, and there was no damage to the submucosal tissues and no ulcer formation. However, in the model group, there were more serious inflammatory cell infiltrations in the colon, the submucosal tissues were broken, and obvious erosion and ulcer formation were observed (Figure 2A). A large number of lymphocytes and monocytes were observed in the mucosa and submucosal layer, the wall of the colon had thickened, and the intrinsic layer of glands was deformed and disorganized in the model group. According to the pathological scoring criteria for ulcerative colitis, compared to the model group, Kuiyangling also significantly reduced the pathological damage score of the intestinal tract in ulcerative mice (Figure 2B). With respect to the Kuiyangling group, colonic damage was evidently decreased in comparison with the model group, and an increased number of lymphocytes and moderate inflammatory cell infiltration were observed. The electron microscopy results indicated that the mucosal glandular structure and mitochondrial structure were normal in the normal group, while the mucosal glandular structure was severely damaged and the mitochondrial membrane was swollen in the model group (Figure 3A). In contrast to the model group, the intestinal mucosal structure was less damaged and the mitochondrial structure was almost normal in the Kuiyangling group. The in vivo imaging results indicated that the intestinal ROS levels were obviously intensified in the model group, when compared to the normal group, while the ROS levels were less intensified in the Kuiyangling group, when compared to the model group (Figure 3B). The results demonstrate that Kuiyangling was able to decrease the destruction of normal intestinal tissues and ROS levels in the UC mice model. The efficacy of mesalazine was similar to that of Kuiyangling.

Transcriptome Analysis of the Intestinal Tract of UC Mice Treated with Kuiyangling

The transcriptional data of each group were evaluated for quality control. It was found that the transcriptional data were valid and reliable and, so, could be used for further analysis (Figure 4A). The transcriptional data of IL1B, citH3, TNF, PAD4, MPO, HUR, ZO1, VDR, Occludin, and Claudin-7 in each group were analyzed, and the results showed that IL1B, citH3, TNF, PAD4, and MPO were increased, while HuR, ZO1, VDR, Occludin, and Claudin-7 were decreased; this trend was reversed after treatment with Kuiyangling, when compared with that in the normal group (Figure 4B). GSEA analysis of KEGG enrichment transcriptional data in the Kuiyangling treatment and model groups revealed that Kuiyangling inhibited the transcriptional levels of the TNF and oxidative phosphorylation signaling pathways, relative to the model group (Figure 4C and D).

GO and KEGG Analysis

The GO (Gene Ontology) and KEGG (Kyoto Encyclopedia of Genes and Genomes) enrichment dissection of different genes in every group indicated that, when compared to the normal group, BP (Biological Process) was mainly enriched in response to the bacterium; CC (Cellular Component) was largely enriched in extracellular space, the collagen-containing extracellular matrix, and extracellular region; and MF (Molecular Function) was chiefly enriched in the extracellular

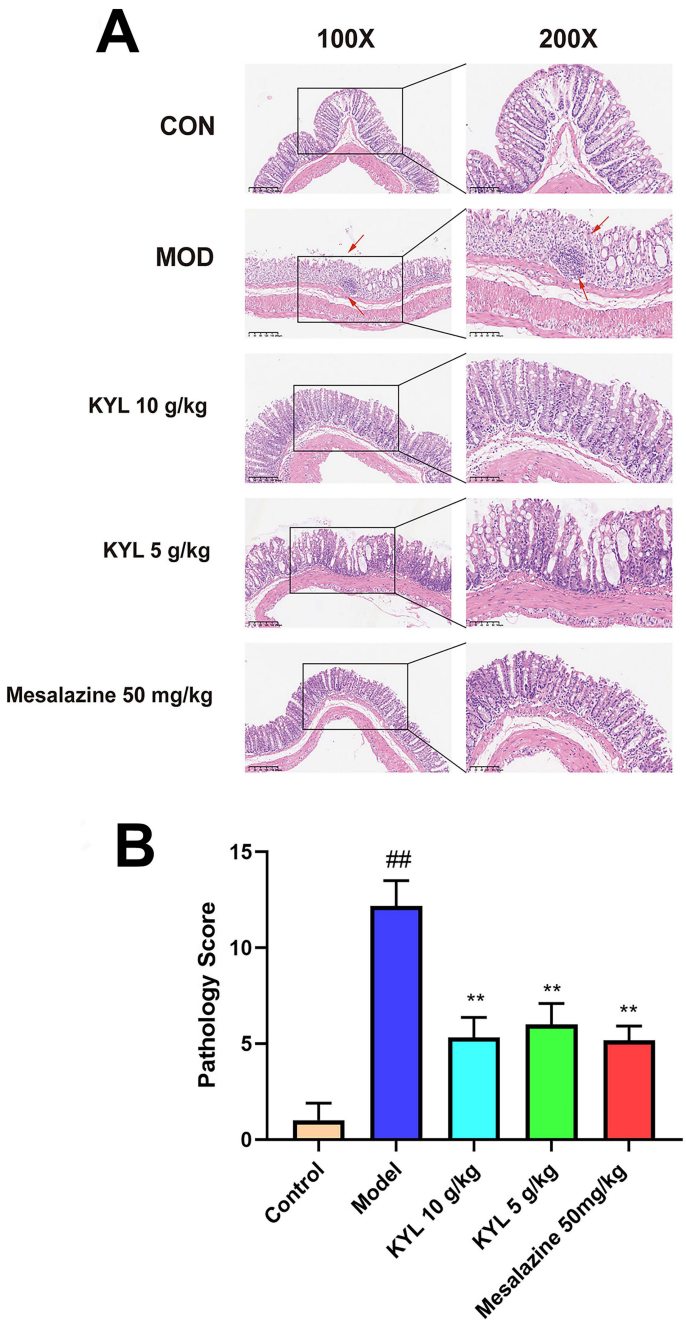

Figure 2 Kuiyangling can maintain the tissue structure of mice with ulcerative colitis. (**A**) Intestinal pathology HE of each group (200×). (**B**) Statistical analysis of intestinal pathological scores between groups. Control, normal group; Model, model group; Mesalazine 50 mg/kg, mesalazine 50 mg/kg group; KYL 5 g/kg, Kuiyangling 5 g/kg group; KYL 10 g/kg, Kuiyangling 10 g/kg group. (##, $P < 0.01$ compared with the normal group; **, $P < 0.01$ compared with the model group).

matrix structural conformation in the model group (Figure 5A). In comparison to the model group, BP was mainly enriched in response to the bacterium; CC was mainly enriched in the brush border membrane, extracellular region, extracellular space, symporter activity, and antagonistic activity; and MF was largely enriched when there is a defensive response to the bacterium in the Kuiyangling treatment group (Figure 5B). In comparison to the model group, BP was mainly concentrated in cellular responses to interferon beta, CC was mainly concentrated in the brush border and symbiont-containing vacuole, and MF was mainly concentrated in GTPase activity1 in the mesalazine treatment group (Figure 5C). In comparison to the normal group, KEGG analysis mainly indicated enrichment in TNF signaling pathway, oxidative phosphorylation, and IL-17 signaling pathway in the model group (Figure 5D). In comparison to the model

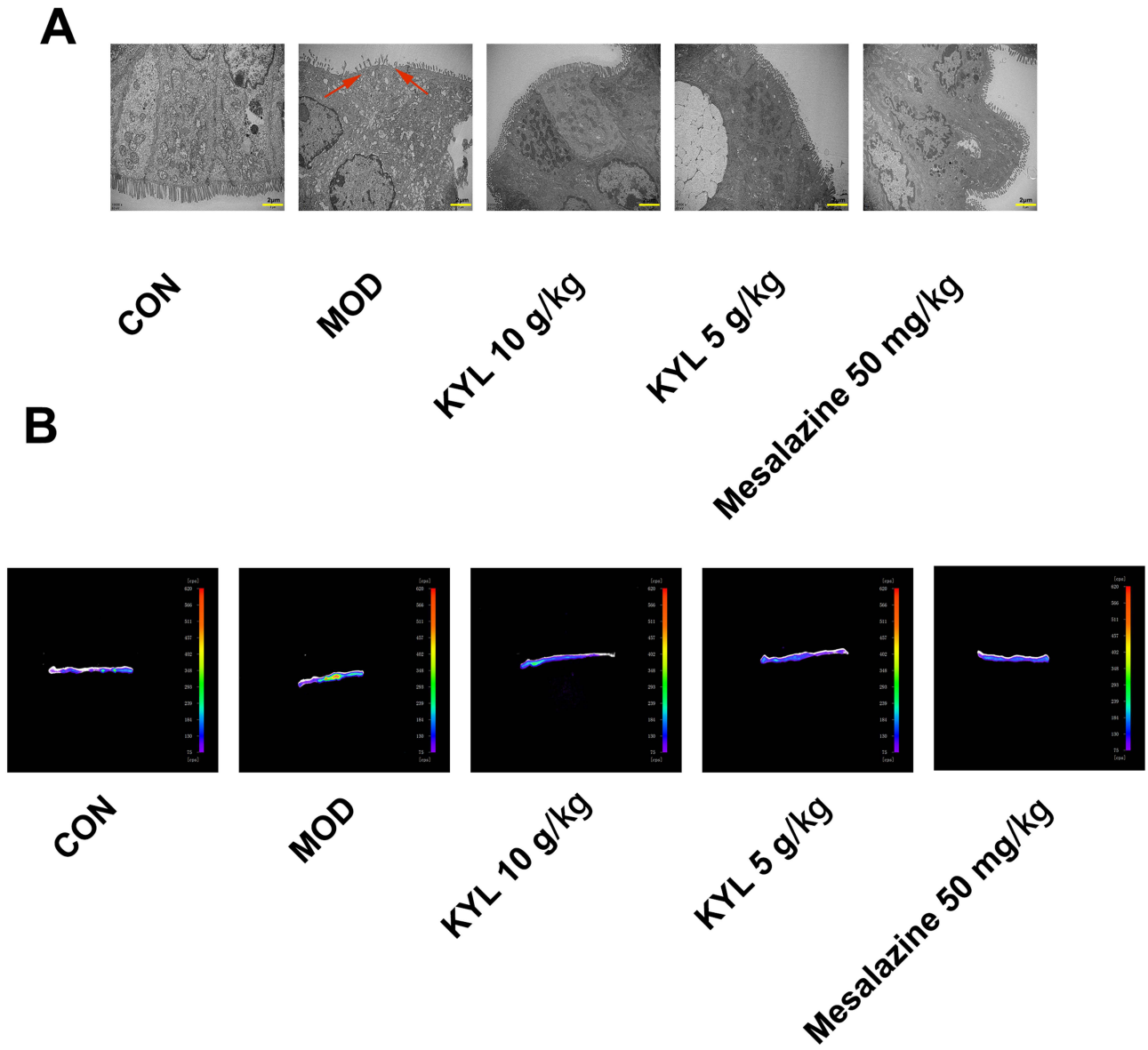

Figure 3 Kuiyangling can reduce the oxidation level of intestinal tissue. (**A**) Electron microscope structure of each group (10,000×). (**B**) ROS imaging of the intestine in each group. CON, normal group; MOD, model group; Mesalazine 50 mg/kg, mesalazine 50 mg/kg group; KYL 5 g/kg, Kuiyangling 5 g/kg group; KYL 10 g/kg, Kuiyangling 10 g/kg group.

group, KEGG enrichment was mainly concentrated in the TNF signaling pathway, NF-kappa B signaling pathway, inflammatory bowel disease, and IL-17 signaling pathway in the Kuiyangling treatment group (Figure 5E). Compared with the model group, KEGG enrichment was mainly concentrated in the TNF signaling pathway, inflammatory bowel disease, IL-17 signaling pathway, PPAR signaling pathway, and NOD-like receiver signaling pathway in the mesalazine treatment group (Figure 5F).

Kuiyangling Can Reduce the Level of NETs in the Intestinal Tissues of UC Mice

With the aim of deeply investigating the mechanism of Kuiyangling when treating UC mice, we checked the NET-related protein expression in the intestinal mucosa tissue. The obtained results indicated that PAD4, citH3, and MPO expression levels were obviously intensified in the model group, compared to the normal group (Figure 6A); however, PAD4, citH3, and MPO expressions were significantly reduced in the Kuiyangling treatment group, when compared to the model group (Figure 6B and C). The content of intestinal NETs in the model group was evidently intensified in comparison to that in

https://doi.org/10.2147/JIR.S492818

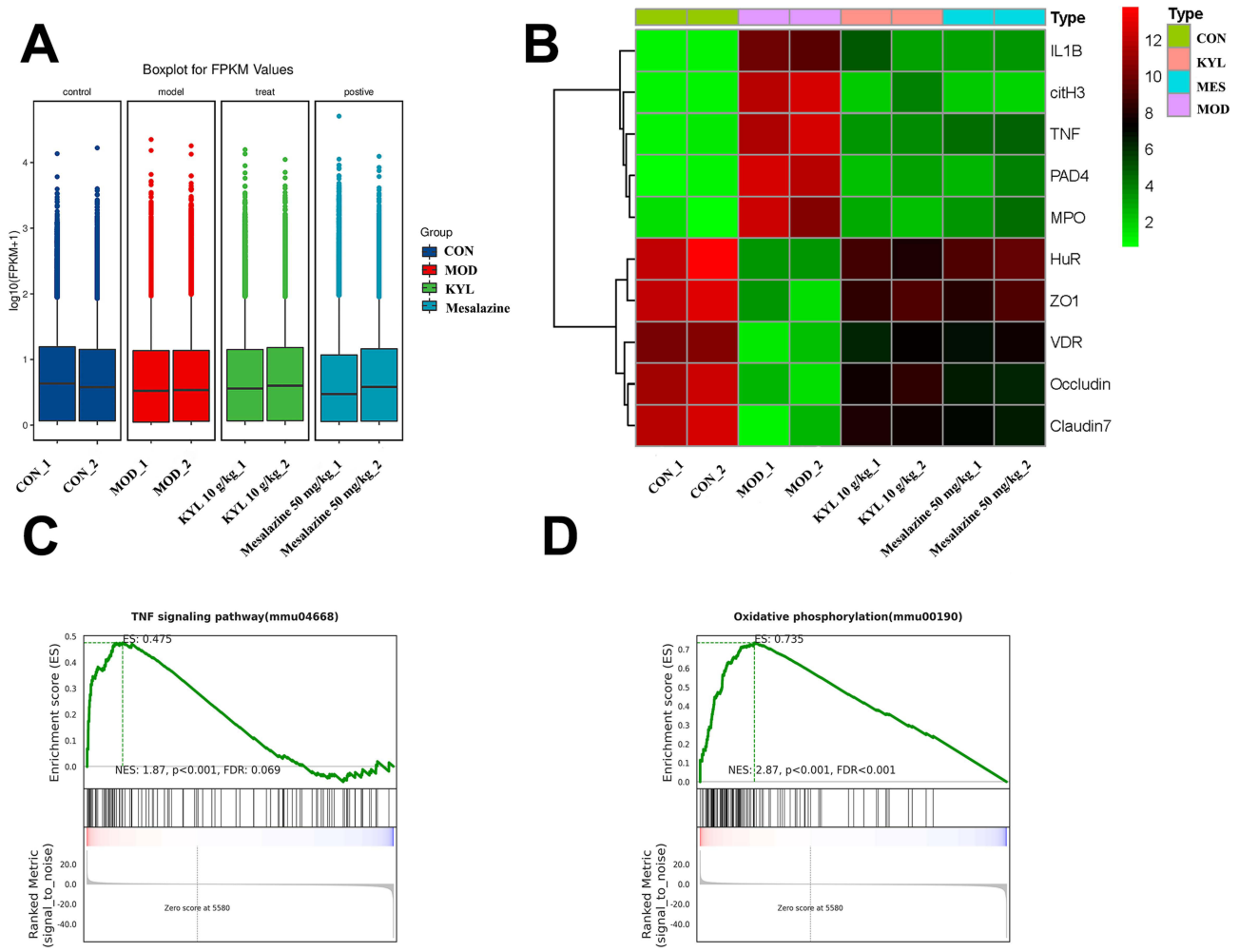

Figure 4 Transcriptome analysis of intestinal mucosal tissue after treatment with Kuiyangling. (**A**) Quality control analysis of transcriptional data for each group. (**B**) Transcription data heatmap of representative proteins. (**C**) and (**D**) GSEA analysis of KEGG signaling pathway enrichment after treatment with Kuiyangling. CON, normal group; MOD, model group; MES, mesalazine 50 mg/kg group; KYL, Kuiyangling 10 g/kg group.

the normal group, while the content of NETs in the Kuiyangling treatment group was significantly decreased in contrast to that in the model group (Figure 6D and E). These results indicate that the mechanism by which Kuiyangling helps to treat UC may be related to a reduction in intestinal NET levels. Meanwhile, the pharmacological effects of mesalazine in UC mice were similar to those of Kuiyangling.

Kuiyangling Can Increase the Expression of HuR/VDR Signaling in the Intestinal Mucosa

As shown in the figure, the immunohistochemistry results revealed that, compared to the normal group, the expression levels of HuR, VDR, ZO-1, Occludin, and Claudin-7 in the colonic mucosa of the model group mice were decreased (Figure 7A and B; Figure 8A–C; Figure 9A–D). However, in the Kuiyangling group, increased expression of HuR, VDR, ZO-1, Occludin, and Claudin-7 was observed in the colonic mucosa of DSS mice. In the HuR/VDR protein complex fluorescent double staining, the immunofluorescence signal of HuR in the colonic mucosal tissue of model group mice was significantly reduced, compared to those in the control group. However, the Kuiyangling group presented enhanced immunofluorescence expression of HuR/VDR in the colonic mucosa of DSS mice. This result is consistent with the immunohistochemistry findings.

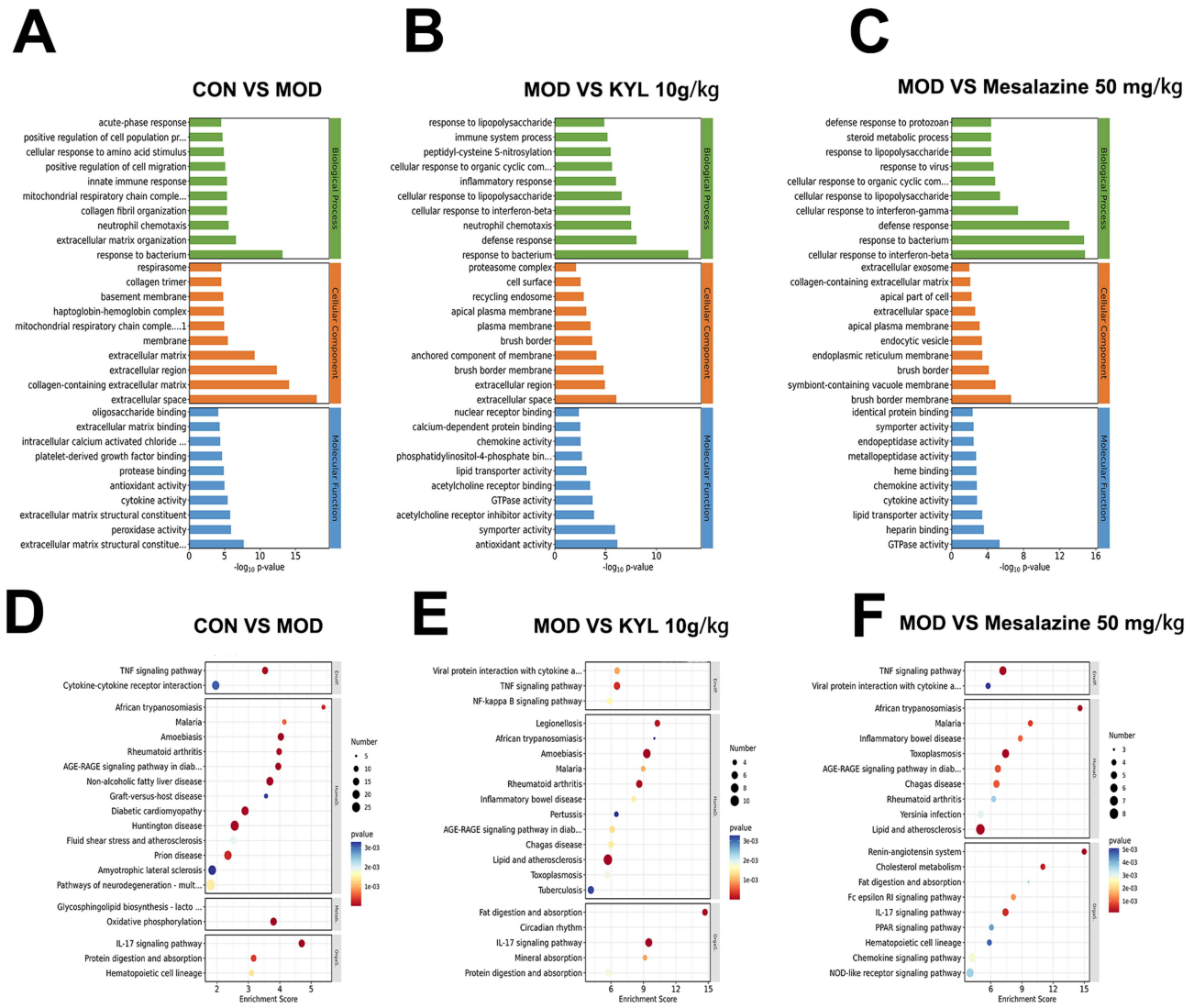

Figure 5 GO and KEGG enrichment analysis of transcriptional data from each group. (**A**) GO enrichment analysis between the normal and model groups. (**B**) GO enrichment analysis between the Kuiyangling 10 g/kg group and the model group. (**C**) GO enrichment analysis between the mesalazine 50mg/kg group and the model group. (**D**) KEGG enrichment analysis between the normal and model groups. (**E**) KEGG enrichment analysis between the Kuiyangling 10 g/kg group and the model group. (**F**) KEGG enrichment analysis between the mesalazine 50mg/kg group and the model group. CON, normal group; MOD, model group; Mesalazine 50 mg/kg, mesalazine 50 mg/kg group; KYL 10 g/kg, Kuiyangling 10 g/kg group.

These results suggest that Kuiyangling has a positive effect, increasing the expression of HuR, VDR, ZO-1, Occludin, and Claudin-7 in the colonic mucosa of the model mice.

Detection of Inflammatory Factors in Peripheral Serum

In comparison to the normal group, the levels of pro-inflammatory elements (IL-1β, IL-6, and TNF-α; Figure 10A–C) were higher and the levels of anti-inflammatory factors (TGF-β, IL-10, and IL-37; Figure 10D–F) were lower in the model group. In contrast to the model group, the levels of pro-inflammatory factors (IL-1β, IL-6, and TNF-α) were higher and the levels of anti-inflammatory factors (TGF-β, IL-10, and IL-37) were lower in the Kuiyangling treatment group. These results indicate that Kuiyangling can reduce the levels of pro-inflammatory elements in the peripheral serum, while enhancing the levels of anti-inflammatory elements.

https://doi.org/10.2147/JIR.S492818

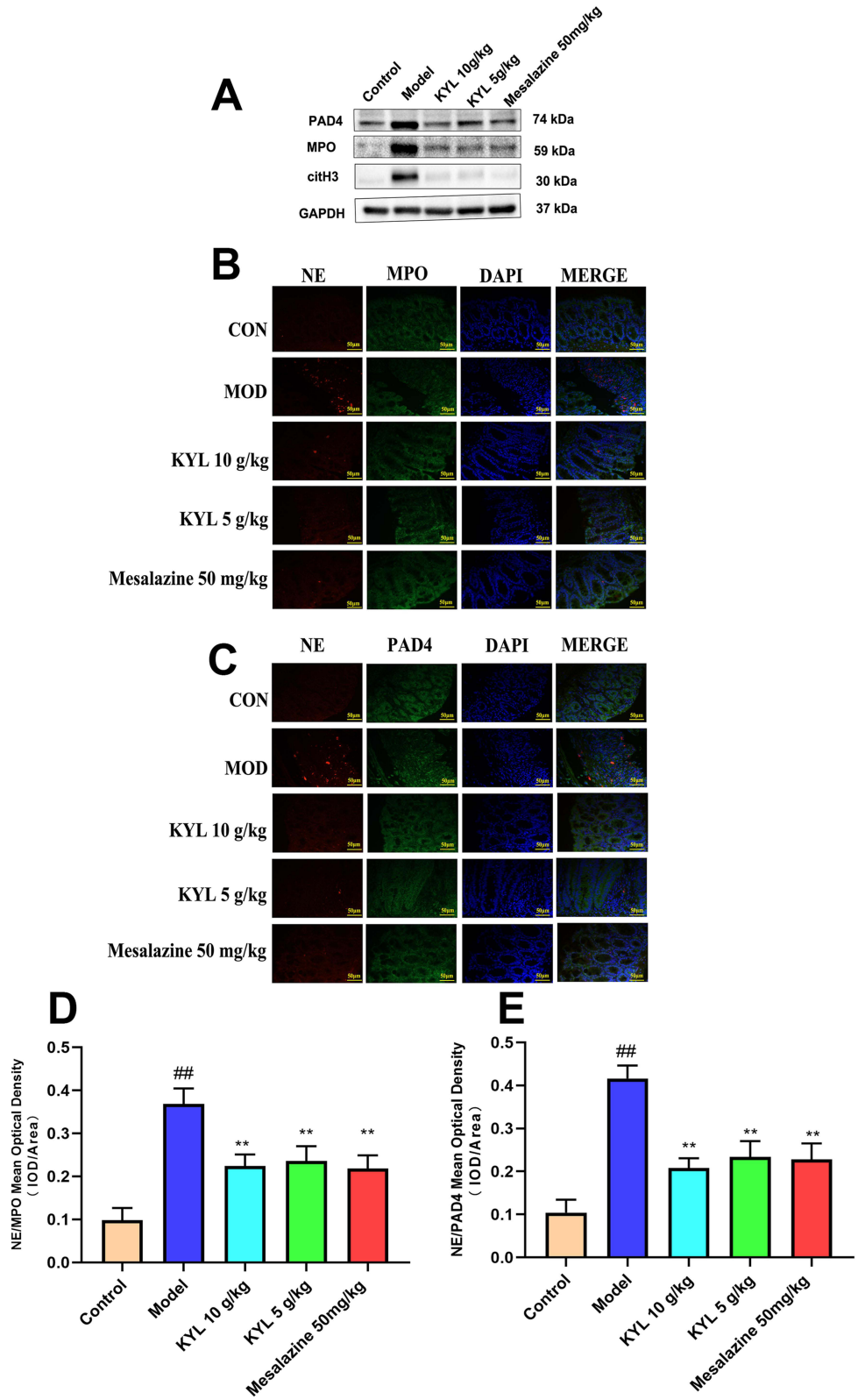

Figure 6 Kuiyangling can reduce the level of intestinal NETs in mice with ulcerative colitis. (**A**) The expression of NET-related proteins (PAD4, MPO, and citH3) in each group. (**B**) and (**D**) NE and MPO in each group were co-stained with immunofluorescence. (**C**) and (**E**) NE and PAD4 in each group were co-stained with immunofluorescence. CON, normal group; MOD, model group; Mesalazine 50 mg/kg, mesalazine 50 mg/kg group; KYL 5 g/kg, Kuiyangling 5 g/kg group; KYL 10 g/kg, Kuiyangling 10 g/kg group. (##, $P < 0.01$ compared with the normal group; **, $P < 0.01$ compared with the model group).

 https://doi.org/10.2147/JIR.S492818

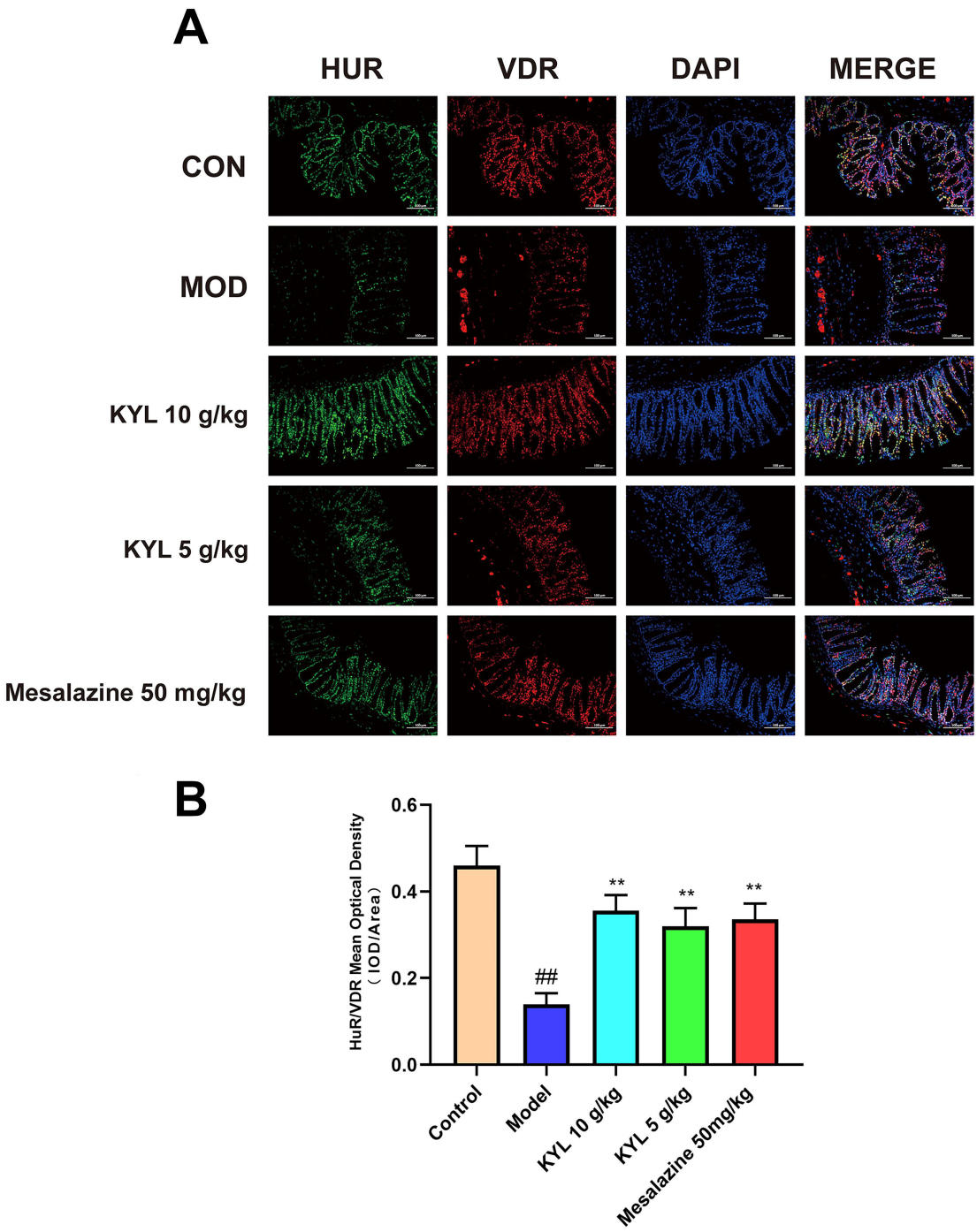

Figure 7 Kuiyangling can increase the expression of HuR/VDR protein complex. (**A**) Immunofluorescence expression of HuR/VDR protein complexes in each group. (**B**) Statistical analysis of the immunofluorescence expression values for HuR/VDR protein complexes in each group. Control, normal group; Model, model group; Mesalazine 50 mg/kg, mesalazine 50 mg/kg group; KYL 5 g/kg, Kuiyangling 5 g/kg group; KYL 10 g/kg, Kuiyangling 10 g/kg group. (##, $P < 0.01$ compared with the normal group; **, $P < 0.01$ compared with the model group).

Discussion

Ulcerative colitis is a long-standing non-specific intestinal inflammatory illness associated with lesions in the intestine mucosa and submucosa.[38] It has the characteristics of a long illness process, recurrent attacks, and can easily become cancerous.[39] At present, the pathogenesis and etiology of UC are not distinct, and there is also a lack of specific therapeutic drugs.[40] Compared with modern medicine, the therapy of ulcerative colitis with traditional Chinese medicines

https://doi.org/10.2147/JIR.S492818

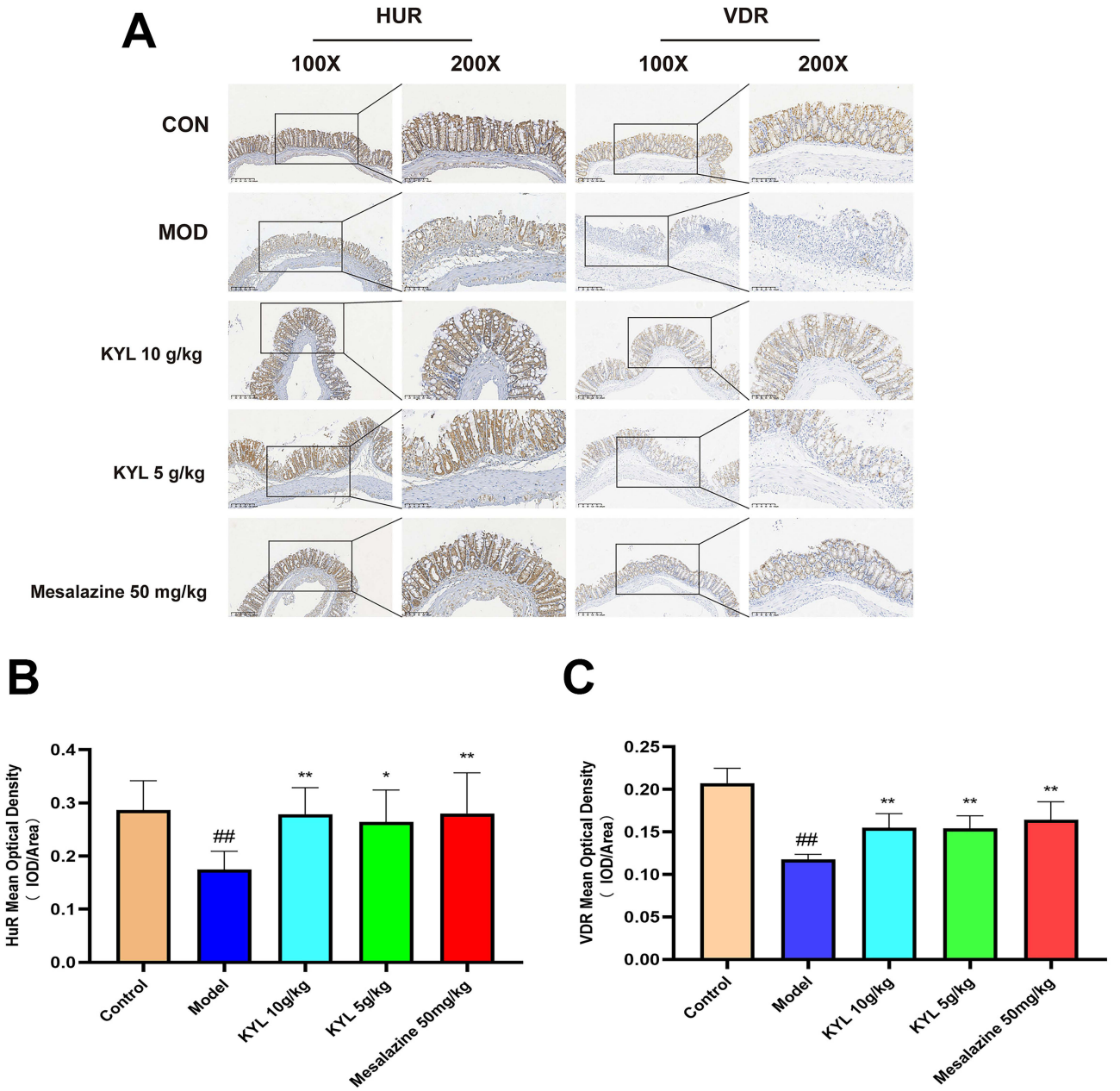

Figure 8 Kuiyangling can promote the expression of HuR and VDR proteins. (**A**) Immunohistochemical expression of HuR and VDR in each group. (**B**) Statistical analysis of HuR immunohistochemical expression in each group. (**C**) Statistical analysis of VDR immunohistochemical expression in each group. Control, normal group; Model, model group; Mesalazine 50 mg/kg, mesalazine 50 mg/kg group; KYL 5 g/kg, Kuiyangling 5 g/kg group; KYL 10 g/kg, Kuiyangling 10 g/kg group. (##, $P < 0.01$ compared with the normal group; *, $P < 0.05$ compared with the model group; **, $P < 0.01$ compared with the model group).

can reduce its recurrence rate, alleviate its symptoms, reduce hormone resistance, and enhance the quality of life of patients; however, their further promotion and application are limited due to the unclear mechanism of action.[41]

The Traditional Chinese Medicine functions of the herbs that compose Kuiyangling are as follows: Kushen clears heat, dries dampness, alleviates itchiness, and detoxifies, while Ercha promotes blood circulation, removes blood stasis, alleviates pain, and aids wound healing. Sanqi stops bleeding, enhances blood circulation, and reduces pain. Baiji stops bleeding, promotes wound healing, removes scar tissue, and nourishes the lungs and yin. Puhuang resolves blood stasis, alleviates pain, and stops bleeding. Huaihua cools the blood, clears liver heat, and reduces fire. Qingdai clears heat, detoxifies, cools the blood, eliminates spots, and calms the nerves. Wubeizi nourishes qi, promotes body fluid production, nourishes the kidney, calms the heart, and has astringent properties. Finally, Baifan strengthens the spleen, invigorates qi,

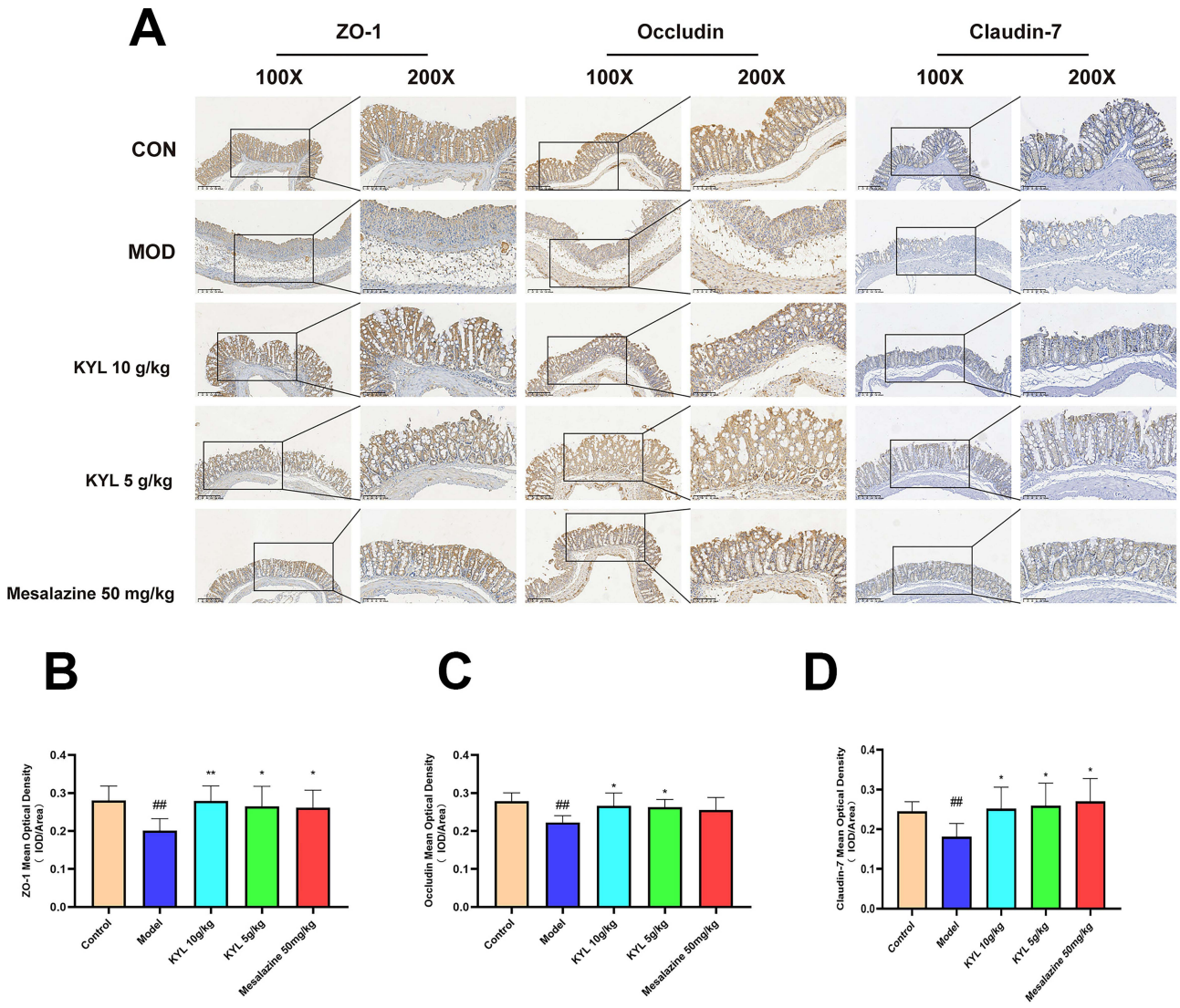

Figure 9 Kuiyangling can promote the expression of ZO1, occludin, and claudin-7. (**A**) Immunohistochemical expression of ZO1, occludin, and claudin-7 in each group. (**B**) Statistical analysis of ZO1 immunohistochemical expression in each group. (**C**) Statistical analysis of occludin immunohistochemical expression in each group. (**D**) Statistical analysis of claudin-7 immunohistochemical expression in each group. Control, normal group; Model, model group; Mesalazine 50 mg/kg, mesalazine 50 mg/kg group; KYL 5 g/kg, Kuiyangling 5 g/kg group; KYL 10 g/kg, Kuiyangling 10 g/kg group. (##, $P < 0.01$ compared with the normal group; *, $P < 0.05$ compared with the model group; **, $P < 0.01$ compared with the model group).

dries dampness, promotes diuresis, stops sweating, and nourishes the fetus. Our group's previous studies have shown that the symptoms of patients with UC in the acute active stage can be significantly reduced through Kuiyangling enema treatment; however, while the treatment mechanism is related to reducing the inflammatory reaction of intestinal tissue, the specific system has not yet been distinguished.[34–37]

In this study, we discovered that Kuiyangling treatment reduced the DAI, spleen index, and ROS content; maintained normal mucosal structure; reduced inflammatory infiltration and mitochondrial damage; and increased the colon length and body weight index in an ulcerative colitis mouse model, when compared to the model group. The obtained results indicate that Kuiyangling is efficient for the therapeutic treatment of ulcerative colitis in vivo. With the objective of deeply investigating the underlying mechanisms, we detected the level of NETs in intestinal mucosa tissues, and observed that the content of NETs in the intestinal mucosa after treatment with Kuiyangling was obviously lower than that in the model group. Western blot analysis also indicated that the level of NET-related proteins decreased significantly after treatment with Kuiyangling. The results demonstrated that the therapeutic mechanism of Kuiyangling is associated with a reduction in the level of NETs. We observed that Kuiyangling decreased the levels of pro-inflammatory elements

https://doi.org/10.2147/JIR.S492818

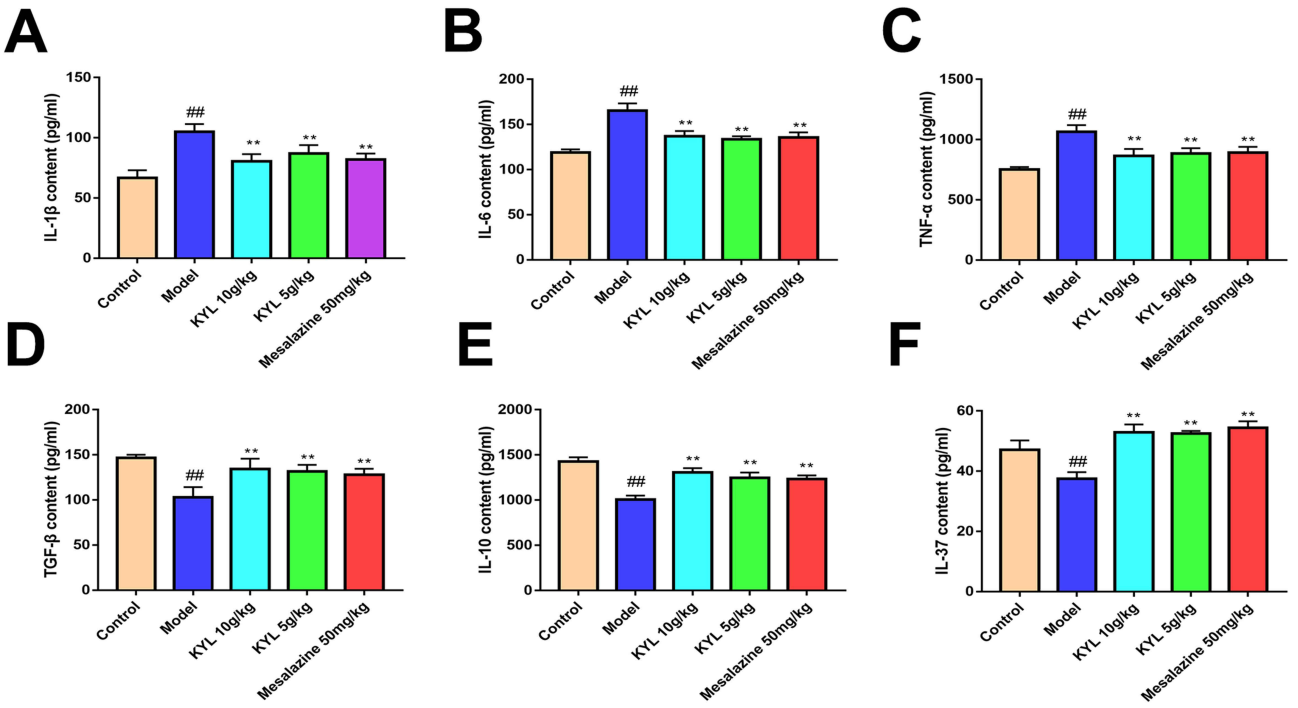

Figure 10 Effect of Kuiyangling on peripheral serum inflammatory factors. (**A**) The content of IL-1β in each group. (**B**) The content of IL-6 in each group. (**C**) The content of TNF-α in each group. (**D**) The content of TGF-β in each group. (**E**) The content of IL-10 in each group. (**F**) The content of IL-37 in each group. CON, normal group; MOD, model group; Mesalazine 50 mg/kg, mesalazine 50 mg/kg group; KYL 5 g/kg, Kuiyangling 5 g/kg group; KYL 10 g/kg, Kuiyangling 10 g/kg group (#, $P < 0.05$ compared with the normal group; ##, $P < 0.01$ compared with the normal group; *, $P < 0.05$ compared with the model group; **, $P < 0.01$ compared with the model group).

and enhanced the levels of anti-inflammatory elements when detecting inflammatory factors in the peripheral blood. These results indicate that Kuiyangling enema not only can reduce the local inflammatory reaction, but also decreases the levels of inflammatory elements in peripheral blood serum, playing a systemic role in efficient treatment.

With the aim of explaining the mechanism by which Kuiyangling can help in treating ulcerative colitis in more depth, we sequenced the transcriptome of intestinal tissues after Kuiyangling enema treatment. Prior to the experiment, we performed an LC-MS analysis of the components of Kuiyangling for quality control. We found that Kuiyangling reduced the transcription levels of inflammatory response proteins, improved the anti-inflammatory response, and maintained intestinal barrier protein levels. The involved signal pathways mainly include the TNF and oxidative phosphorylation signaling pathways. From another perspective, Kuiyangling enhanced the expression of the downstream mucosal barrier proteins ZO-1, Occludin, and Claudin-7 through promoting the expression of HuR/VDR signals, thus promoting repair of the intestinal mucosa after injury.

The above results demonstrate that Kuiyangling can reduce the level of intestinal NETs, promote the expression of HuR/VDR signaling, and inhibit the TNF and oxidative phosphorylation signaling pathways to alleviate the symptoms of ulcerative colitis.

Neutrophils can release NETs in two forms: suicidal NETs and vital NETs.[42] The suicidal NETs depend on NADPH. When neutrophils are stimulated by PMA, the calcium ions in the endoplasmic reticulum are released into the cytoplasm, and the increase in calcium ions in the cytoplasm activates PKC. Then, phosphorylated Gp91phox activates NADPH oxidase to produce ROS.[43] At the same time, the elevated calcium ion level in the cytoplasm can activate peptidyl arginine deaminase 4 (PAD4), which can produce arginine residues on citrullinated histones, leading to chromatin de-polymerization.[44] Elevated ROS levels induce MPO and NE located in the nucleus, further de-polymerizing the chromatin. This process is accompanied with the destruction of the nuclear and cell membranes, leading to an interaction between DNA and the cytoplasmic protein, which is then released into the extracellular space to form NETs.[45] This process takes at least 2 to 6 hours, and PAD4 is the key enzyme. As such, inhibiting PAD4 can block the formation of NETs. The vital NETs only take from 5 to 60 minutes to form. This process is not accompanied by destruction of the cell

membrane and does not depend on ROS. The two types of NETs produce different stages, in terms of NET formation times; however, eventually, NETs can induce neutrophils to form NETosis. ROS play a pivotal part in the formation of NETosis. A few research studies have shown that blocking ROS can significantly reduce the occurrence of NETosis and reduce the damage to tissues induced by NETs.[46] In this study, we also performed live imaging of intestinal ROS and observed that Kuiyangling reduced the production of intestinal ROS. Moreover, Kuiyangling also significantly inhibited the expression of PAD4 proteins.

NETs are the key to innate immunity.[47] Nevertheless, apart from providing protection for bodies, NETs also participate in the occurrence and advancement of disease.[48] Research studies have shown that the excessive accumulation of NETs or damage to NET clearance systems (ie, NETs imbalance) might exert severe impacts upon bodies.[48] First, the components of NETs, including DNA, granular protein, and histone, can serve as the host's auto-antigen, introducing auto-immune illnesses. Second, NETs that cannot be completely degraded in the blood or tissue may cause capillary obstruction, damage to the microcirculation of the body, and even tissue damage, leading to various diseases such as thrombosis, cystic fibrosis, and septicemia.[49] Therefore, NETs are a double-edged sword: on one hand, NETs can kill pathogenic micro-organisms; on the other hand, the imbalance of NET clearance will aggravate the chronic inflammation of the body, leading to organ damage.[50]

Many types of parasites, fungi, and bacteria discovered within human intestinal tissue have been proved to arouse the formation of NETs.[51] It is undeniable that NETs play a defensive role in resisting bacterial invasion. Some studies have found that the content of NETs in the intestinal tissue of IBD patients was increased, when compared with normal tissue, and the NETs content significantly decreased after treatments.[52] DNase—a NETs scavenger— significantly reversed the damage of DSS in the intestine of mice.[16] The co-culture pattern of activated neutrophils and enteroid Caco-2 cells indicated that NETs might cause intestinal epithelial cell damage by means of a local straightforward contact between their associated proteases and intestinal epithelial cells.[53] A research study has demonstrated that the F-actin cytoskeleton of human intestinal epithelioid cells was damaged, and this damage can be reversed through inhibiting the release of proteases on NETs.[54] In addition, a study has found that, in a model of bacterial enteritis, NETs can cause the pathogens Shiga toxin-producing *Escherichia coli* (STEC) and enteropathogenic *Escherichia coli* (EPEC) to attach to the intestinal mucosa via the DNA chain, thus causing damage to the intestinal mucosa.[55] In addition, *Escherichia coli* strains can absorb extracellular DNA and use it as nutrients to promote their growth, leading to intestinal flora disorder. The levels of pentapeptide-related proteins (PTX3), MPO, and NE have been explored inside the colon mucosa of patients suffering from UC (ulcerative colitis),[16] which are also components of NETs. Although these molecules may be secreted independently from NETs, the obtained data support the view that NETs participate in UC. The pathogenesis of these NET components in UC patients may be due to the role of NETs in promoting coagulation, increasing the incidence of intestinal thromboembolism in UC patients and exacerbating the progression of UC.[56] In addition, NETs can directly induce cell apoptosis, and it is possible to reduce their local concentration in the intestine and reduce their toxic effects.[57] NETs can also damage intestinal microvascular endothelial cells, increase microvascular permeability, and cause tissue edema and oxidative damage.[15]

In IBD, the TNF signal is secreted through the Th1 cell's α mediation. In addition to secreting TNF-α, Th1 cells can secrete IL-1 and IL-6.[58] These cytokines can concentrate granulocytes inside the intestine. The neutrophils gathered inside the intestine produce NETs, induced by external factors, which will induce more inflammatory factors (eg, TNF- α, IL-1, and IL-6) and eventually lead to intestinal matrix degradation, epithelial injury, endothelial activation, and vascular destruction.[59] Clinical research has shown that anti-TNF treatment can promote the mucosal healing of IBD patients, reduce hospitalization and surgery, and improve the quality of life of patients.[60] The efficacy of anti-TNF-α drugs has been supported by a large amount of clinical evidence, and they are highly accessible for patients,[61] making them classic biological agents that dominate the IBD market. Excessive oxidative stress in intestinal tissue is an important factor in the aggravation of inflammatory bowel disease (IBD).[62] ROS produced through the oxidative phosphorylation signal pathway can aggravate mucosal damage and the inflammatory reaction of IBD intestinal tissues.[63] ROS are an important link in the formation of NETs. In turn, excessive NETs aggravate ROS production and amplify the oxidative phosphorylation signal pathway.[43] NETs, the TNF signaling pathway, and the oxidative phosphorylation signaling pathway all present positive feedback with respect to each other.[16]

Damage to the intestinal mucosa and the impairment of barrier function are important pathological mechanisms and clinical manifestations of inflammatory bowel disease (IBD). Mucosal damage can lead to barrier dysfunction and induce mucosal inflammation. HuR is a post-transcriptional regulator of intestinal epithelial homeostasis, which plays a role in regulating cell proliferation, migration, apoptosis, and autophagy.[64] VDR is a highly expressed nuclear receptor in the intestinal epithelium, which intervenes in various downstream genes through binding specifically with ligands.[65] Clinical studies in IBD patients have shown significantly decreased levels of HuR and VDR in their intestinal mucosa, associated with mucosal repair and barrier disruption. Dysregulation of the HuR/VDR pathway is involved in the process of mucosal damage and delayed healing in IBD patients, where the mechanism involves HuR directly regulating the translation of VDR, thereby regulating the rapid recovery of the epithelium after injury. HuR/VDR can also further regulate downstream markers, such as the expression of tight junction proteins ZO-1, Occludin, and Claudin-7, affecting epithelial barrier function. In addition, HuR/VDR also play roles in regulating the expression of inflammatory factors, modulating immune responses, and influencing the gut microbiota, thus maintaining the homeostasis of the intestinal mucosa. Previous studies have shown that Kuiyangling can promote restoration of the intestinal mucosa in UC patients. In this study, it was found that Kuiyangling improved the expression levels of HuR, VDR, ZO-1, Occludin, and Claudin-7 in the colonic mucosa in a DSS-induced mouse model. In summary, the mechanism by which Kuiyangling can help to treat UC may be related to the HuR/VDR-mediated intestinal mucosal barrier repair.

One limitation of our study is the relatively small number of some experiments conducted. While we have carefully designed and executed our experiment to ensure the validity of our results, the lack of multiple experiments limits the generalizability of our findings and increases the risk of error or bias. Previous research in this field has often used a larger number of experiments to validate their findings, and we acknowledge that this would strengthen the conclusions of our study.

Given the complexity of Kuiyangling's ingredients, further verification was carried out through comparisons with reference compounds and literature searches. The total ion chromatogram is presented in the Supplementary Figure 1, and the specific identification results are detailed in the Supplementary Table 1. After identification and screening, the following compounds are identified as the main components of Kuiyangling. These components may play significant pharmacological roles. These compounds are as follows: Ginsenoside Rb1, lsomer of Indirubin, Indirubin, Matrine, Sophocarpine, Oxysophocarpine, Oxymatrine, Epigallocatechin, Epicatechin, Cianidanol, Typhaneoside, Rutin, Gallic acid, Notoginsenoside R1, Ginsenoside Rg1, Quercetin. In our future work, we can focus on validating the effects and mechanisms of these compounds in treating ulcerative colitis through enema administration.

Future research could address this limitation by conducting additional experiments with a larger sample size. Alternatively, alternative methods such as quantitative PCR or mass spectrometry could be used to validate our findings. Despite this limitation, we believe that our study provides valuable insights into the mechanisms of Kuiyangling in treating ulcerative colitis The rigor of our experimental design and the novelty of our findings demonstrate the potential impact of our research on the field.

The mechanism by which NETs are involved in intestinal functional injuries is very complex, and there exist few relevant research studies. Therefore, elaboration of the detailed and exact mechanism of NET-mediated intestinal injury still requires further study. The excessive formation and/or reduction in clearance of NETs may promote inflammation, auto-immune diseases, vascular diseases, thrombosis, ischemia-reperfusion injury, and the growth and metastasis of tumors, as well as participating in a variety of pathological injuries. Therefore, reducing the formation of NETs and the release of their components is helpful for controlling certain pathological injuries and inflammatory diseases. These measures have been proven to be effective in animal models and provide a promising treatment approach. In this study, Kuiyangling not only reduced the production of NETs, but also inhibited the TNF and oxidative phosphorylation signaling pathways, demonstrating that Kuiyangling acts on ulcerative colitis by affecting multiple pathways and targets. However, this study lacked further validation in patients and research content for specific targets. In the future, we intend to further improve the level of evidence regarding the effect of Kuiyangling on ulcerative colitis by conducting RCT (randomized controlled trial) research and assessing the mechanisms in specifically targeted knockout mice in order to refine the relevant signal pathways.

Conclusion

Kuiyangling enema demonstrated potential efficacy in treating ulcerative colitis in mice, associated with a reduction in intestinal NETs and enhancement of HuR-mediated intestinal barrier signaling pathways.

Data Sharing Statement

The data used in this study have been securely stored and are available for access by other researchers upon reasonable request. For detailed information regarding data access, please contact the authors for further guidance. We are committed to promoting transparency and replicability in scientific research to support academic sharing and collaboration.

Acknowledgments

I would like to express my sincere gratitude to my supervisors and colleagues for their invaluable guidance and support throughout the course of this research. Additionally, I acknowledge the facilities and resources provided by our laboratory, which were instrumental in the successful completion of this study.

Funding

This research was supported by Guangdong Basic and Applied Basic Research Foundation (2022A1515110851), Shenzhen Science and Technology Program (JCYJ20220531092005011), National Natural Science Foundation of China, (82305105), National Natural Science Foundation of China (82204994), and Sanming Project of Medicine in Shenzhen (No. SZZYSM202211002).

Disclosure

The authors do not have any possible conflicts of interest.

References

1. Kobayashi T, Siegmund B, Le Berre C. et al. Ulcerative colitis. *Nat Rev Dis Primers*. 2020;6(1):74. doi:10.1038/s41572-020-0205-x
2. Feuerstein JD, Moss AC, Farraye FA. Ulcerative Colitis. *Mayo Clin Proc*. 2019;94(7):1357–1373. doi:10.1016/j.mayocp.2019.01.018
3. Segal JP, LeBlanc JF, Hart AL. Ulcerative colitis: an update. *Clin Med Lond*. 2021;21(2):135–139. doi:10.7861/clinmed.2021-0080
4. Du L, Ha C. Epidemiology and Pathogenesis of Ulcerative Colitis. *Gastroenterol Clin North Am*. 2020;49(4):643–654. doi:10.1016/j.gtc.2020.07.005
5. Kuenzig ME, Fung SG, Marderfeld L, et al. Twenty-first Century Trends in the Global Epidemiology of Pediatric-Onset Inflammatory Bowel Disease: systematic Review. *Gastroenterology*. 2022;162(4):1147–1159.e4. doi:10.1053/j.gastro.2021.12.282
6. Antia C, Baquerizo K, Korman A, Bernstein JA, Alikhan A. Urticaria: a comprehensive review: epidemiology, diagnosis, and work-up. *J Am Acad Dermatol*. 2018;79(4):599–614. doi:10.1016/j.jaad.2018.01.020
7. Kucharzik T, Koletzko S, Kannengiesser K, Dignass A. Ulcerative Colitis-Diagnostic and Therapeutic Algorithms. *Dtsch Arztebl Int*. 2020;117(33–34):564–574. doi:10.3238/arztebl.2020.0564
8. Lasa JS, Olivera PA, Danese S, Peyrin-Biroulet L. Efficacy and safety of biologics and small molecule drugs for patients with moderate-to-severe ulcerative colitis: a systematic review and network meta-analysis. *Lancet Gastroenterol Hepatol*. 2022;7(2):161–170. doi:10.1016/S2468-1253(21)00377-0
9. Ho GT, Cartwright JA, Thompson EJ, Bain CC, Rossi AG. Resolution of Inflammation and Gut Repair in IBD: translational Steps Towards Complete Mucosal Healing. *Inflamm Bowel Dis*. 2020;26(8):1131–1143. doi:10.1093/ibd/izaa045
10. Burgener SS, Schroder K. Neutrophil Extracellular Traps in Host Defense. *Cold Spring Harb Perspect Biol*. 2020;12(7):a037028. doi:10.1101/cshperspect.a037028
11. de Bont CM, Boelens WC, Pruijn GJM. NETosis, complement, and coagulation: a triangular relationship. *Cell Mol Immunol*. 2019;16(1):19–27. doi:10.1038/s41423-018-0024-0
12. Papayannopoulos V. Neutrophil extracellular traps in immunity and disease. *Nat Rev Immunol*. 2018;18(2):134–147. doi:10.1038/nri.2017.105
13. Friedrich M, Pohin M, Jackson MA, et al. IL-1-driven stromal-neutrophil interactions define a subset of patients with inflammatory bowel disease that does not respond to therapies. *Nat Med*. 2021;27(11):1970–1981. doi:10.1038/s41591-021-01520-5
14. Dos Santos Ramos A, Viana GCS, de Macedo Brigido M, Almeida JF. Neutrophil extracellular traps in inflammatory bowel diseases: implications in pathogenesis and therapeutic targets. *Pharmacol Res*. 2021;171:105779. doi:10.1016/j.phrs.2021.105779
15. Li T, Wang C, Liu Y, et al. Neutrophil Extracellular Traps Induce Intestinal Damage and Thrombotic Tendency in Inflammatory Bowel Disease. *J Crohn's Colitis*. 2020;14(2):240–253. doi:10.1093/ecco-jcc/jjz132
16. Dinallo V, Marafini I, Di Fusco D, et al. Neutrophil Extracellular Traps Sustain Inflammatory Signals in Ulcerative Colitis. *J Crohn's Colitis*. 2019;13(6):772–784. doi:10.1093/ecco-jcc/jjy215
17. Angelidou I, Chrysanthopoulou A, Mitsios A, et al. REDD1/Autophagy Pathway Is Associated with Neutrophil-Driven IL-1β Inflammatory Response in Active Ulcerative Colitis. *J Immunol*. 2018;200(12):3950–3961. doi:10.4049/jimmunol.1701643

18. Hu Y, Ye Z, She Y, et al. Efficacy and Safety of Probiotics Combined With Traditional Chinese Medicine for Ulcerative Colitis: a Systematic Review and Meta-Analysis. *Front Pharmacol*. 2022;13:844961. doi:10.3389/fphar.2022.844961
19. Zheng S, Xue T, Wang B, Guo H, Liu Q. Chinese Medicine in the Treatment of Ulcerative Colitis: the Mechanisms of Signaling Pathway Regulations. *Am J Chin Med*. 2022;50(7):1781–1798. doi:10.1142/S0192415X22500756
20. Majumder M, Chakraborty P, Mohan S, Mehrotra S, Palanisamy V. HuR as a molecular target for cancer therapeutics and immune-related disorders. *Adv Drug Deliv Rev*. 2022;188:114442. doi:10.1016/j.addr.2022.114442
21. Xiao L, Li XX, Chung HK, et al. RNA-Binding Protein HuR Regulates Paneth Cell Function by Altering Membrane Localization of TLR2 via Post-transcriptional Control of CNPY3. *Gastroenterology*. 2019;157(3):731–743. doi:10.1053/j.gastro.2019.05.010
22. Sharma S, Xiao L, Wang JY. HuR and Its Interactions with Noncoding RNAs in Gut Epithelium Homeostasis and Diseases. *Front Biosci*. 2023;28 (10):262. doi:10.31083/j.fbl2810262
23. Wu X, Xu L. The RNA-binding protein HuR in human cancer: a friend or foe? *Adv Drug Deliv Rev*. 2022;184:114179. doi:10.1016/j.addr.2022.114179
24. Liu L, Christodoulou-Vafeiadou E, Rao JN, et al. RNA-binding protein HuR promotes growth of small intestinal mucosa by activating the Wnt signaling pathway. *Mol Biol Cell*. 2014;25(21):3308–3318. doi:10.1091/mbc.e14-03-0853
25. Liu L, Zhuang R, Xiao L, et al. HuR Enhances Early Restitution of the Intestinal Epithelium by Increasing Cdc42 Translation. *Mol Cell Biol*. 2017;37(7). doi:10.1128/MCB.00574-16
26. Carlberg C. Vitamin D and Its Target Genes. *Nutrients*. 2022;14(7):1354. doi:10.3390/nu14071354
27. Aggeletopoulou I, Marangos M, Assimakopoulos SF, Mouzaki A, Thomopoulos K, Triantos C. Vitamin D and Microbiome: molecular Interaction in Inflammatory Bowel Disease Pathogenesis. *Am J Pathol*. 2023;193(6):656–668. doi:10.1016/j.ajpath.2023.02.004
28. Battistini C, Ballan R, Herkenhoff ME, Saad SMI, Sun J. Vitamin D Modulates Intestinal Microbiota in Inflammatory Bowel Diseases. *Int J Mol Sci*. 2020;22(1):362. doi:10.3390/ijms22010362
29. Wu S, Zhang YG, Lu R, et al. Intestinal epithelial vitamin D receptor deletion leads to defective autophagy in colitis. *Gut*. 2015;64(7):1082–1094. doi:10.1136/gutjnl-2014-307436
30. Pagnini C, Di Paolo MC, Graziani MG, Delle Fave G. Probiotics and Vitamin D/Vitamin D Receptor Pathway Interaction: potential Therapeutic Implications in Inflammatory Bowel Disease. *Front Pharmacol*. 2021;12:747856. doi:10.3389/fphar.2021.747856
31. White JH. Vitamin D deficiency and the pathogenesis of Crohn's disease. *J Steroid Biochem Mol Biol*. 2018;175:23–28. doi:10.1016/j.jsbmb.2016.12.015
32. Zhang Y, Cai JZ, Xiao L, et al. RNA-binding protein HuR regulates translation of vitamin D receptor modulating rapid epithelial restitution after wounding. *Am J Physiol Cell Physiol*. 2020;319(1):C208–c217. doi:10.1152/ajpcell.00009.2020
33. Sun J, Zhang YG. Vitamin D Receptor Influences Intestinal Barriers in Health and Disease. *Cells*. 2022;11(7):1129. doi:10.3390/cells11071129
34. Feng C, Zhang Q, Chen X, Mu G, Huang M. Clinical observation on the treatment of ulcerative colitis with oral Chinese medicine and enema and its effect on IL-6 and IL-10 in intestinal mucosa. *J Emergency Traditional Chin Med*. 2013;22(11):1878–1880.
35. Xiaorong C, Minghe H. Observation on the treatment of ulcerative colitis with anal dropping Kuiyangling. *Clin J Traditional Chin Med*. 2014;26 (03):271–272.
36. Yabin W. Treatment of ulcerative colitis with modified Kuiyangling retention enema. *Pract Clin J Integrat Tradition Chin Western Med*. 2018;18 (01):83–84.
37. Yabin W, Minghe H. Observation on the treatment of ulcerative colitis of the sigmoid colon and rectum with Kuiyangling. *Clin J Traditional Chin Med*. 2019;31(04):733–735.
38. Spinelli A, Bonovas S, Burisch J, et al. ECCO Guidelines on Therapeutics in Ulcerative Colitis: surgical Treatment. *J Crohn's Colitis*. 2022;16 (2):179–189. doi:10.1093/ecco-jcc/jjab177
39. Adams SM, Close ED, Shreenath AP. Ulcerative Colitis: rapid Evidence Review. *Am Fam Physician*. 2022;105(4):406–411.
40. Krugliak Cleveland N, Torres J, Rubin DT. What Does Disease Progression Look Like in Ulcerative Colitis, and How Might It Be Prevented? *Gastroenterology*. 2022;162(5):1396–1408. doi:10.1053/j.gastro.2022.01.023
41. Liu Y, Li BG, Su YH, et al. Potential activity of Traditional Chinese Medicine against Ulcerative colitis: a review. *J Ethnopharmacol*. 2022;289:115084. doi:10.1016/j.jep.2022.115084
42. Guillotin F, Fortier M, Portes M, et al. Vital NETosis vs. suicidal NETosis during normal pregnancy and preeclampsia. *Front Cell Dev Biol*. 2022;10:1099038. doi:10.3389/fcell.2022.1099038
43. Ravindran M, Khan MA, Palaniyar N. Neutrophil Extracellular Trap Formation: physiology, Pathology, and Pharmacology. *Biomolecules*. 2019;9 (8):365. doi:10.3390/biom9080365
44. Monteith AJ, Miller JM, Beavers WN, et al. Mitochondrial Calcium Uniporter Affects Neutrophil Bactericidal Activity during Staphylococcus aureus Infection. *Infect Immun*. 2022;90(2):e0055121. doi:10.1128/iai.00551-21
45. Brostjan C, Oehler R. The role of neutrophil death in chronic inflammation and cancer. *Cell Death Discov*. 2020;6(1):26. doi:10.1038/s41420-020-0255-6
46. Hu M, Li H, Li G, et al. NETs promote ROS production to induce human amniotic epithelial cell apoptosis via ERK1/2 signaling in spontaneous preterm birth. *Am J Reprod Immunol*. 2023;89(3):e13656. doi:10.1111/aji.13656
47. Tan C, Aziz M, Wang P. The vitals of NETs. *J Leukoc Biol*. 2021;110(4):797–808. doi:10.1002/JLB.3RU0620-375R
48. Mutua V, Gershwin LJ. A Review of Neutrophil Extracellular Traps (NETs) in Disease: potential Anti-NETs Therapeutics. *Clin Rev Allergy Immunol*. 2021;61(2):194–211. doi:10.1007/s12016-020-08804-7
49. Fousert E, Toes R, Desai J. Neutrophil Extracellular Traps (NETs) Take the Central Stage in Driving Autoimmune Responses. *Cells*. 2020;9(4):915. doi:10.3390/cells9040915
50. Castanheira FVS, Kubes P. Neutrophils and NETs in modulating acute and chronic inflammation. *Blood*. 2019;133(20):2178–2185. doi:10.1182/blood-2018-11-844530
51. Kumar S, Gupta E, Kaushik S, Jyoti A. Neutrophil Extracellular Traps: formation and Involvement in Disease Progression. *Iran J Allergy Asthma Immunol*. 2018;17(3):208–220.
52. Drury B, Hardisty G, Gray RD, Ho GT. Neutrophil Extracellular Traps in Inflammatory Bowel Disease: pathogenic Mechanisms and Clinical Translation. *Cell Mol Gastroenterol Hepatol*. 2021;12(1):321–333. doi:10.1016/j.jcmgh.2021.03.002

53. Lai HJ, Doan HT, Lin EY, et al. Histones of Neutrophil Extracellular Traps Directly Disrupt the Permeability and Integrity of the Intestinal Epithelial Barrier. *Inflamm Bowel Dis*. 2023;29(5):783–797. doi:10.1093/ibd/izac256
54. Marin-Esteban V, Turbica I, Dufour G, et al. Afa/Dr diffusely adhering Escherichia coli strain C1845 induces neutrophil extracellular traps that kill bacteria and damage human enterocyte-like cells. *Infect Immun*. 2012;80(5):1891–1899. doi:10.1128/IAI.00050-12
55. Crane JK, Broome JE, Lis A. Biological Activities of Uric Acid in Infection Due to Enteropathogenic and Shiga-Toxigenic Escherichia coli. *Infect Immun*. 2016;84(4):976–988. doi:10.1128/IAI.01389-15
56. He Z, Si Y, Jiang T, et al. Phosphotidylserine exposure and neutrophil extracellular traps enhance procoagulant activity in patients with inflammatory bowel disease. *Thromb Haemost*. 2016;115(4):738–751. doi:10.1160/TH15-09-0710
57. Silvestre-Roig C, Braster Q, Wichapong K, et al. Externalized histone H4 orchestrates chronic inflammation by inducing lytic cell death. *Nature*. 2019;569(7755):236–240. doi:10.1038/s41586-019-1167-6
58. Schmitt H, Neurath MF, Atreya R. Role of the IL23/IL17 Pathway in Crohn's Disease. *Front Immunol*. 2021;12:622934. doi:10.3389/fimmu.2021.622934
59. An Z, Li J, Yu J, et al. Neutrophil extracellular traps induced by IL-8 aggravate atherosclerosis via activation NF-kappaB signaling in macrophages. *Cell Cycle*. 2019;18(21):2928–2938. doi:10.1080/15384101.2019.1662678
60. Cui G, Fan Q, Li Z, Goll R, Florholmen J. Evaluation of anti-TNF therapeutic response in patients with inflammatory bowel disease: current and novel biomarkers. *EBioMedicine*. 2021;66:103329. doi:10.1016/j.ebiom.2021.103329
61. Gisbert JP, Chaparro M. Predictors of Primary Response to Biologic Treatment [Anti-TNF, Vedolizumab, and Ustekinumab] in Patients With Inflammatory Bowel Disease: from Basic Science to Clinical Practice. *J Crohn's Colitis*. 2020;14(5):694–709. doi:10.1093/ecco-jcc/jjz195
62. Bourgonje AR, Feelisch M, Faber KN, Pasch A, Dijkstra G, van Goor H. Oxidative Stress and Redox-Modulating Therapeutics in Inflammatory Bowel Disease. *Trends Mol Med*. 2020;26(11):1034–1046. doi:10.1016/j.molmed.2020.06.006
63. Zhou J, Li M, Chen Q, et al. Programmable probiotics modulate inflammation and gut microbiota for inflammatory bowel disease treatment after effective oral delivery. *Nat Commun*. 2022;13(1):3432. doi:10.1038/s41467-022-31171-0
64. Liu X, Xiao L, Wang JY. Posttranscriptional control of intestinal epithelium homeostasis by RNA-binding protein HuR. *Sheng Li Xue Bao*. 2020;72(3):325–335.
65. Kellermann L, Jensen KB, Bergenheim F, et al. Mucosal vitamin D signaling in inflammatory bowel disease. *Autoimmun Rev*. 2020;19(11):102672. doi:10.1016/j.autrev.2020.102672